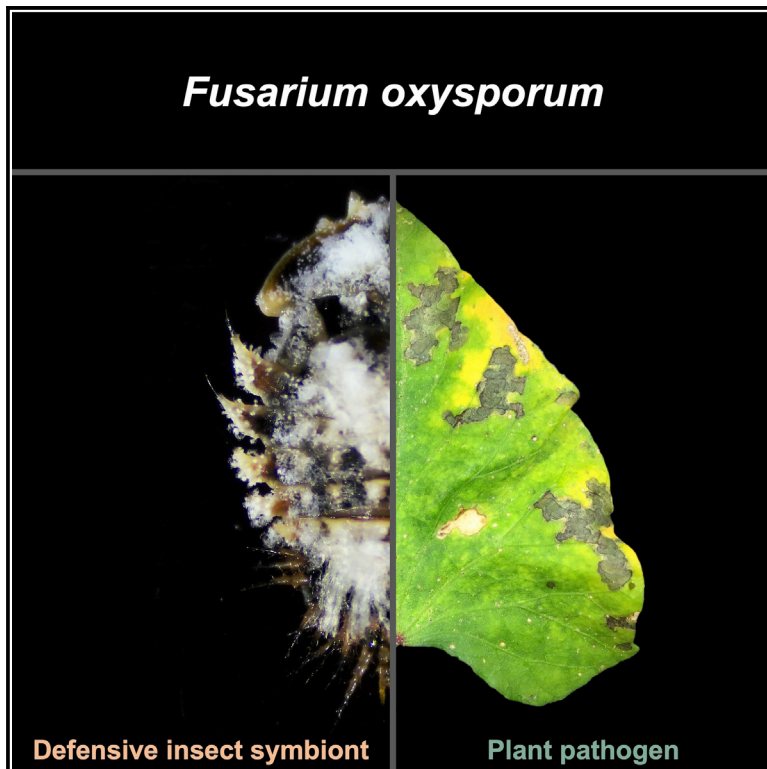


# Current Biology

## The leaf beetle *Chelymorpha alternans* propagates a plant pathogen in exchange for pupal protection

### Graphical abstract



### Authors

Aileen Berasategui, Noa Breitenbach, Marleny García-Lozano, ..., Nadine Ziemert, Donald Windsor, Hassan Salem

### Correspondence

aileen.berasategui-lopez@uni-tuebingen.de (A.B.), hassan.salem@tuebingen.mpg.de (H.S.)

### In brief

Holometabolous insects must contend with antagonistic challenges during the immobile pupal stage. Berasategui et al. reveal that tortoise beetles rely on pupal protection from their fungal symbiont, *Fusarium oxysporum*. In exchange, the beetle propagates the fungus to naive host plants, extending the infection range of this plant pathogen.

### Highlights

- Tortoise leaf beetles engage in mutualism with the ascomycete *Fusarium oxysporum*
- The fungus confers pupal protection for the beetle against predation
- Beetles propagate *F. oxysporum* to their host plants, causing wilt disease
- Symbiont genome is reduced but retained features that reflect its dual lifestyle

Article

# The leaf beetle *Chelymorpha alternans* propagates a plant pathogen in exchange for pupal protection

Aileen Berasategui,<sup>1,2,7,\*</sup> Noa Breitenbach,<sup>1</sup> Marleny García-Lozano,<sup>1</sup> Inès Pons,<sup>1</sup> Brigitte Sailer,<sup>3</sup> Christa Lanz,<sup>4</sup> Viterbo Rodríguez,<sup>5</sup> Katharina Hipp,<sup>3</sup> Nadine Ziemert,<sup>2</sup> Donald Windsor,<sup>6</sup> and Hassan Salem<sup>1,8,9,\*</sup>

<sup>1</sup>Max Planck Institute for Biology, Mutualisms Research Group, Max-Planck-Ring 5, Tübingen 72076, Germany

<sup>2</sup>University of Tübingen, Cluster of Excellence ‘Controlling Microbes to Fight Infections’, Auf der Morgenstelle 28, Tübingen 72076, Germany

<sup>3</sup>Max Planck Institute for Biology, Electron Microscopy Facility, Max-Planck-Ring 5, Tübingen 72076, Germany

<sup>4</sup>Max Planck Institute for Biology, Genome Center, Max-Planck-Ring 5, Tübingen 72076, Germany

<sup>5</sup>Centro Regional Universitario de Veraguas, Centro de Capacitación, Investigación y Monitoreo de la Biodiversidad en Coiba, Calle Décima, vía San Francisco, Santiago 08001, Republic of Panama

<sup>6</sup>Smithsonian Tropical Research Institute, Luis Clement Avenue, Bldg. 401 Tupper, Panama City 0843-03092, Republic of Panama

<sup>7</sup>Twitter: @Berasymbionts

<sup>8</sup>Twitter: @HassanSalem

<sup>9</sup>Lead contact

\*Correspondence: [aileen.berasategui-lopez@uni-tuebingen.de](mailto:aileen.berasategui-lopez@uni-tuebingen.de) (A.B.), [hassan.salem@tuebingen.mpg.de](mailto:hassan.salem@tuebingen.mpg.de) (H.S.)

<https://doi.org/10.1016/j.cub.2022.07.065>

## SUMMARY

Many insects rely on microbial protection in the early stages of their development. However, in contrast to symbiont-mediated defense of eggs and young instars, the role of microbes in safeguarding pupae remains relatively unexplored, despite the susceptibility of the immobile stage to antagonistic challenges. Here, we outline the importance of symbiosis in ensuring pupal protection by describing a mutualistic partnership between the ascomycete *Fusarium oxysporum* and *Chelymorpha alternans*, a leaf beetle. The symbiont rapidly proliferates at the onset of pupation, extensively and conspicuously coating *C. alternans* during metamorphosis. The fungus confers defense against predation as symbiont elimination results in reduced pupal survivorship. In exchange, ecdysing beetles vector *F. oxysporum* to their host plants, resulting in a systemic infection. By causing wilt disease, the fungus retained its phytopathogenic capacity in light of its symbiosis with *C. alternans*. Despite possessing a relatively reduced genome, *F. oxysporum* encodes metabolic pathways that reflect its dual lifestyle as a plant pathogen and a defensive insect symbiont. These include virulence factors underlying plant colonization, along with mycotoxins that may contribute to the defensive biochemistry of the insect host. Collectively, our findings shed light on a mutualism predicated on pupal protection of an herbivorous beetle in exchange for symbiont dissemination and propagation.

## INTRODUCTION

Antagonistic interactions are widespread in nature,<sup>1</sup> exerting strong selective pressures to evolve protective traits.<sup>2–4</sup> Among insects, symbioses with beneficial microbes serve as a rich source of defensive adaptations.<sup>5</sup> Symbiont-mediated protection can stem from competitively excluding pathogens and parasites<sup>6,7</sup> by priming the immune system against potential infections<sup>8,9</sup> or through the production of bioactive compounds that promote the defensive biochemistry of the host.<sup>10,11</sup>

Similar to obligate nutritional partnerships,<sup>12,13</sup> a number of defensive mutualisms are faithfully transmitted and exhibit a high degree of evolutionary stability.<sup>14–19</sup> The fixation of a protective symbiont within its host’s population can reflect the temporal and spatial persistence of predatory, parasitic, or pathogenic threats, justifying the metabolic cost of symbiosis.<sup>20,21</sup> Across beetles,<sup>22,23</sup> wasps,<sup>24</sup> and bugs,<sup>16</sup> symbiont-mediated protection is typically described for eggs and juvenile stages that are at a greater risk to antagonistic challenges. However,

despite the prevalence of defensive mutualisms in insects,<sup>24,23–25</sup> the role of symbiotic microbes in protecting the pupal stage remains undescribed for most holometabolous clades.<sup>5,26</sup>

The risk of parasitism and predation can be high for pupae,<sup>27–32</sup> serving as a selective force for counteradaptations that ensure survivorship during metamorphosis. Although insectivorous birds and rodents can and do feed on pupae,<sup>33,34</sup> most threats seem to arise from non-visual predators and parasitoids such as ground beetles, ants, and wasps.<sup>35</sup> As such, physical and chemical adaptations offer refuge for insects to evade antagonistic challenges.<sup>36</sup> These include spinning cocoons or silk nets prior to metamorphosis,<sup>37</sup> where filaments protect the enclosed pupa. Spines and secretory hairs are similarly effective,<sup>38</sup> either by deterring physical contact or by actively exuding defensive secretions that are unpalatable to potential predators.<sup>39</sup> Here, we extend this narrative by highlighting the role of symbiotic microbes in conferring pupal protection, using the tortoise leaf beetle *Chelymorpha alternans* (Coleoptera:Chrysomelidae:Cassidinae) as a study system.

Cassidines represent a highly diverse subfamily of leaf beetles that includes more than 6,000 species.<sup>40</sup> The ecological radiation of tortoise beetles and their capacity to exploit a diverse range of angiosperms is tied to the origin of a symbiosis with *Candidatus Stammera capleta*, a pectin-degrading bacterial symbiont maintained in specialized organs near the foregut.<sup>41–43</sup> In addition to *Stammera*, *C. alternans* and other cassidines are hosts to reproductive manipulators such as *Wolbachia*<sup>44</sup> and *Spiroplasma*,<sup>44</sup> highlighting the range of interactions with microbial symbionts across the subfamily and their impact on host development and ecology. Although the life cycle and general morphology of *C. alternans* resembles that of many herbivorous beetles, it differs in that the pupal stage is covered by a conspicuous white substance (Figure 1A).<sup>45</sup> Earlier reports described the substance as a waxy secretion or flocculence,<sup>45</sup> resembling those produced by scale insects. In this study, we reveal this substance to be largely fungal (Figures 1B and 1C). Through microscopy and molecular and genomic characterizations, along with bioassays in the laboratory and field, we detail a symbiosis that confers pupal protection in a beetle in exchange for symbiont dispersal and propagation.

## RESULTS AND DISCUSSION

### *Fusarium oxysporum*, a fungal symbiont of *Chelymorpha alternans*

We explored the microbial community associated with *C. alternans* pupae through metagenome sequencing and profiled its composition using phyloFlash v.3.4.<sup>46</sup> By screening for and retrieving the small subunit ribosomal RNA gene (SSU rRNA), our analysis assigned 854 rRNA sequences spanning bacteria, archaea, and fungi. We observe that pupae are hosts to previously described bacterial symbionts in *C. alternans*,<sup>41,44</sup> including *Stammera* and *Wolbachia*, in addition to a mycobiome composed entirely of *Fusarium oxysporum* (Table S1). This is in line with culture-dependent approaches pointing to *F. oxysporum* as the only microbe consistently isolated from the fibrous growths on the outer surfaces of pupae. To characterize the prevalence of *F. oxysporum* across beetle development, we performed diagnostic PCR in eggs, larvae, pupae, in addition to adult males and females. *F. oxysporum* is universally present throughout the life cycle of *C. alternans* (Table S2), which is indicative of a stable and faithfully transmitted symbiosis with its beetle host.

To resolve the phylogenetic position of *C. alternans*-associated *F. oxysporum* relative to representative ascomycetes, a phylogenomic tree was constructed on the basis of 180 marker genes (Data S5). A maximum-likelihood analysis confirmed the placement of the beetle's symbiont alongside other strains of *F. oxysporum*, and part of a species complex composed of pathogenic and nonpathogenic lineages. Our analysis revealed that the symbiont of *C. alternans* is most closely related to fungi that are causal to wilt disease in cabbage, broccoli, radish, and cotton, forming a well-supported monophyly (Figure 1D; Data S5).

### Rapid symbiont proliferation following pupation

As dense filamentous aggregations of *F. oxysporum* appear to form immediately on the surface of the *C. alternans* following pupation (Figures 1B and 1C), we aimed to describe the symbiont's

population dynamics throughout the developmental stage by applying qPCR targeting the microbe's *Tef-1 $\alpha$*  gene. We observe a thousand-fold increase in symbiont abundance between days 1 and 2 post-pupation, followed by a highly stable population spanning the remaining 5 days required for *C. alternans* to complete metamorphosis (Figure 2) (linear model [LM],  $F_{5,12} = 6.04$ ,  $p = 0.005$ ; Data S1). The rapid growth of *F. oxysporum* early in pupal development, followed by a conserved presence throughout its duration (Figure 2), is suggestive of a stage-specific role that may be required during this immobile phase.

### Symbiont-mediated pupal protection

We hypothesized that *F. oxysporum* may confer a protective benefit to its beetle host, given its conspicuous cuticular localization (Figures 1B and 1C) and rapid proliferation at the onset of pupation (Figure 2). Like many tropical insects, *C. alternans* experiences strong antagonistic pressures by ants, nematodes, and assassin bugs, in addition to parasitoid wasps and flies.<sup>45</sup> Cassidinae larvae contend with these challenges by constructing fecal shields that provide chemical and physical protection.<sup>40,45,47</sup> Additionally, the evolution of maternal care in a subset of tortoise beetle species ensures that immature stages, including pupae, are defended throughout development against natural predators.<sup>47,48</sup> However, beyond emitting lateral rhythmic movements when disturbed, *C. alternans* pupae lack both defensive adaptations,<sup>45</sup> highlighting the susceptibility of this phase and the potential role of *F. oxysporum* in alleviating antagonistic threats.

To generate symbiont-free *C. alternans* (Figure 3A), we treated the external surfaces of newly pupated insects with 0.5% (w/v) benzimidazole solution (5 g benzimidazole/100 mL H<sub>2</sub>O), a demonstrated fungicide against a range of fusaria.<sup>49</sup> The efficacy of this treatment was assessed by symbiont-specific qPCR (Figure 3B), revealing marked suppression in symbiont abundance relative to untreated pupae (unpaired Wilcoxon rank-sum test,  $W = 2$ ,  $p = 0.001$ ). Adult eclosion rates under laboratory conditions were consistently high across both groups (91% [CI = 73%–97%] benzimidazole-treated; 95% [CI = 79%–99%] untreated control; generalized linear model [GLM, binomial],  $\chi^2 = 0$ ,  $df = 1$ ,  $p = 1$ ) (Figure 3C), indicating that the topical application of benzimidazole did not adversely affect insect development within the pupal case.

To assess the role of *F. oxysporum* as a defensive symbiont, field experiments were conducted in the natural environment of *C. alternans* in Gamboa, Republic of Panamá (N: 9°07'12.5; W: 79°41'46.0). Pupae were either applied with benzimidazole as described above or left untreated. Both groups were then separated into cages that were either exposed or sealed, yielding four experimental treatments in total (Figure 3D). Survival rates were compared across all groups and throughout 4 days. Benzimidazole-treated pupae reared in exposed cages suffered a higher predation rate relative to untreated pupae, as well as pupae treated with the fungicide but maintained in sealed cages (Figure 3D) (log-rank test,  $\chi^2 = 34.8$ ,  $df = 3$ ,  $p < 0.001$ ; Cox's model,  $p < 0.001$ ; Data S1). In contrast, untreated pupae in exposed cages exhibited a similar survivorship rate relative to the two experimental groups maintained in sealed cages (Figure 3D; Data S1), highlighting the protective role of *F. oxysporum* for its beetle host. As ants are among the most abundant and impactful

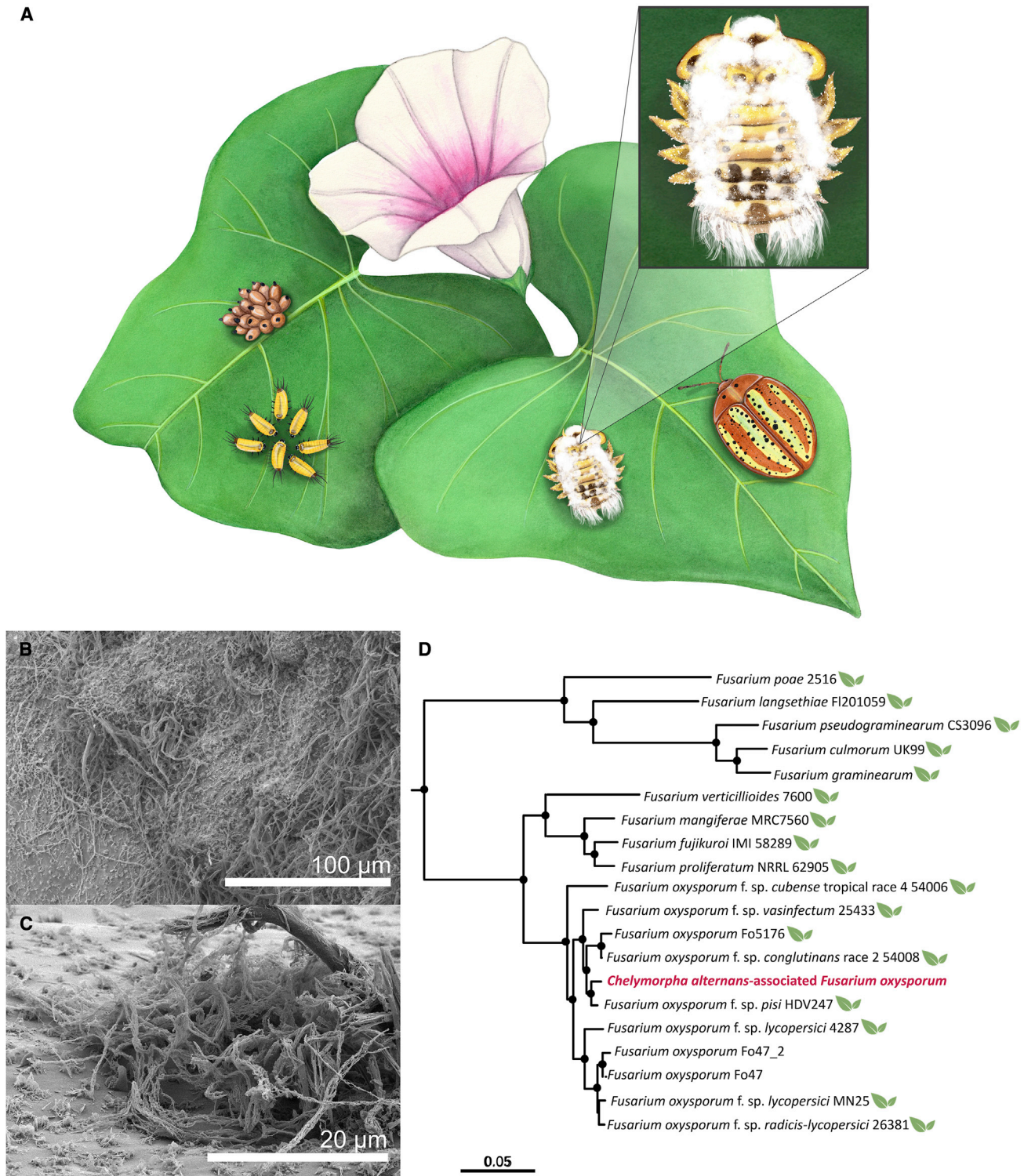


**Figure 1. Symbiosis between the tortoise beetle *Chelymorpha alternans* and *Fusarium oxysporum***

(A) Illustration depicting the life cycle and different developmental stages of *C. alternans*, including eggs, larvae, pupa, and an adult beetle (direction counter-clockwise) on the sweet potato plant, *Ipomoea batatas*. A pupa illustrates the dense filamentous growth of *F. oxysporum* on the pupa.

(B and C) Scanning electron microscopy image of the exterior surface of the pupal case and the fungal symbiont. Scale bars are included for reference.

(D) Maximum-likelihood phylogeny based on 180 concatenated genes revealing the phylogenetic placement of the *C. alternans*-associated *F. oxysporum* (red) relative to other members of the species complex and the *Fusarium* genus. Node coloration reflects bootstrap support >95%. Leafy icon indicates plant pathogenic lineages. This is an abridged version. See also [Data S5](#) and [Tables S1](#) and [S2](#).

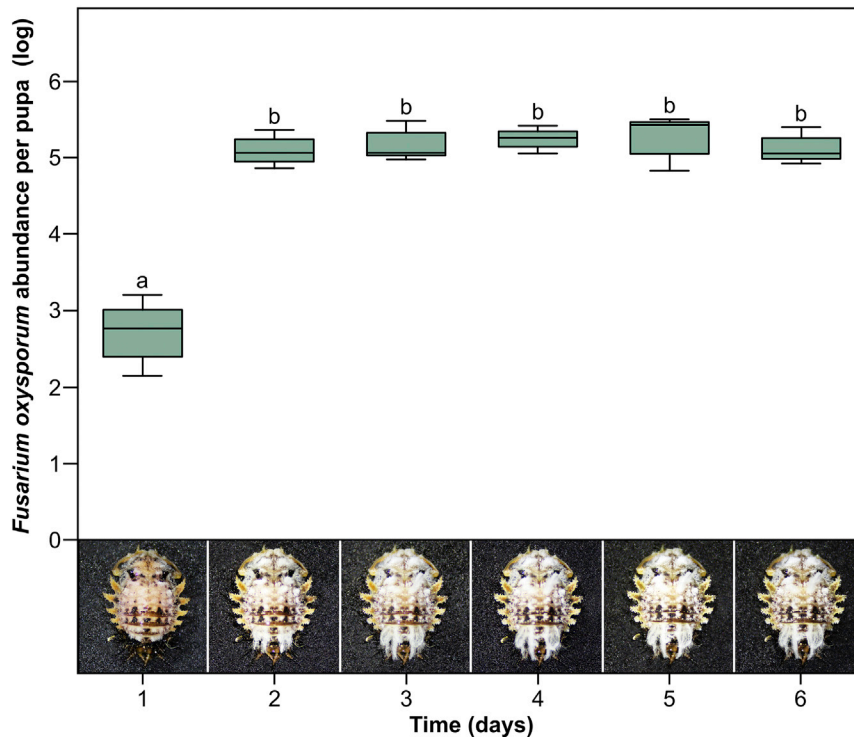


**Figure 2. *Fusarium oxysporum* rapidly proliferates at the onset of pupation**

Symbiont population dynamics during pupal development following the quantification of Tef-1 $\alpha$  gene copy numbers ( $n = 18$ ; LM,  $F_{5,12} = 6.04$ ,  $p = 0.005$ ; [Data S1](#)). Lines represent medians, boxes comprise the 25–75 percentiles, and whiskers denote the range. Images reflect a time series of a single pupa throughout the 6 days required for *C. alternans* to complete metamorphosis. Different letters above boxes indicate significant differences.

implicated in a variety of plant diseases that include wilts, blights, and rots.<sup>58,59</sup> Members of the speciose genus impact both natural and managed ecosystems and employ a broad range of infection strategies that can either initiate in roots from soilborne populations or invade leaves and stems following contact with spore-bearing vectors.<sup>58</sup>

As tortoise beetles typically transition to a different feeding site following pupation,<sup>40,45</sup> we asked whether *C. alternans* can vector *F. oxysporum* to naive sweet

predators on the ground and in lower vegetation in tropical rain forests,<sup>50</sup> we surveyed ant communities within a 4-m radius from the experiment's site. This revealed a consortium composed of carpenter ants (*Camponotus senex*) and generalist species, *Azteca lacrymosa* and *A. chartiex*. The latter two are noteworthy, given the predacious habits of *Azteca* ants on Casidinae pupae,<sup>50</sup> including *C. alternans*<sup>45</sup> ([Video S1](#)). Owing to the possible inhibitory and off target effects of some fungicides, future efforts will capitalize on the development of additional symbiont-clearing protocols to generate stable aposymbiotic populations of *C. alternans*.

Symbiont-mediated protection is described across a number of diverse insect clades.<sup>16,22–25,51–53</sup> Many of these mutualisms feature soil-dwelling taxa that run a higher risk of pathogenic infection or groups that are vulnerable to antagonistic threats early in development. Beewolves provision antibiotic-producing *Streptomyces* in brood cells,<sup>53</sup> thereby ensuring the protection of progeny from mold fungi during their month-long development in underground nests.<sup>24</sup> Symbiont protection extends beyond pathogenic threats and can counter predation by other arthropods, as demonstrated in rove beetles.<sup>54–56</sup> The production of pederin, a potent amid toxin, in eggs and larvae is a function of its defensive symbiont, *Pseudomonas*.<sup>54</sup> Larvae hatching from pederin-free eggs experience increased predation relative to symbiotic insects that are chemically defended,<sup>56</sup> a dynamic that may govern the partnership between tortoise beetles and *F. oxysporum*.

### Eclosing beetles propagate *F. oxysporum* to naive host plants

Time-calibrated phylogenies indicate that fusaria originated and diversified with flowering plants  $\sim 91.3$  mya,<sup>57</sup> where they are

potato plants (*Ipomoea batatas*), one of several convolvulaceous vines on which it thrives.<sup>60</sup> The exposure of *I. batatas* to newly eclosed *C. alternans* revealed that the beetle does indeed propagate its fungal symbiont to previously uninfected plants ([Figure 4A](#)) (Pearson's  $\chi^2$  test,  $\chi^2 = 5.95$ ,  $df = 1$ ,  $p = 0.01$ ), resulting in a systemic infection as confirmed through diagnostic PCR using *F. oxysporum*-specific primers. Similar to other holometabolous insects, *C. alternans* emerges from its pupal skin by actively peeling it with its tarsal pads and claws.<sup>45</sup> Thus, the beetle's legs, representing the first point of contact between a recently eclosed adult and a new plant, may be contaminated with symbiont spores after shedding *F. oxysporum*-rich exuviae. We quantified *F. oxysporum* titers in the appendages of *C. alternans* (spanning the coxa to the tarsal claws) and found that symbiont density on legs is largely representative of adult beetles as a whole ([Figure 4B](#)) (LM,  $F_{1,4} = 0.48$ ,  $p = 0.53$ ). Scanning electron microscopy further revealed that the beetle's tarsal pads, and its associated setae, bear fragmented microbial aggregations that may stem from the symbiont population coating the pupal skin ([Figures 4C–4F](#)).

Beetles are important vectors of numerous plant pathogens owing to their impressive diversity spanning nearly all terrestrial ecosystems,<sup>61–64</sup> and the key role of herbivory in fueling their ecological radiation.<sup>65,66</sup> The epidemiology of these microbes, spanning eukaryotic and prokaryotic clades, is dependent on the population dynamics and dispersal of their beetle hosts.<sup>64</sup> Darkling beetles (Coleoptera:Tenebrionidae) transmit *Burkholderia gladioli* to soybean plants, in exchange for microbe-mediated protection of an immobile stage (in this case, the egg).<sup>22</sup> Ambrosia beetles belonging to the *Euwallacea* genus (Coleoptera:Curculionidae:Scolytinae) cultivate and consume a range of fusaria, which they, in turn, disseminate to

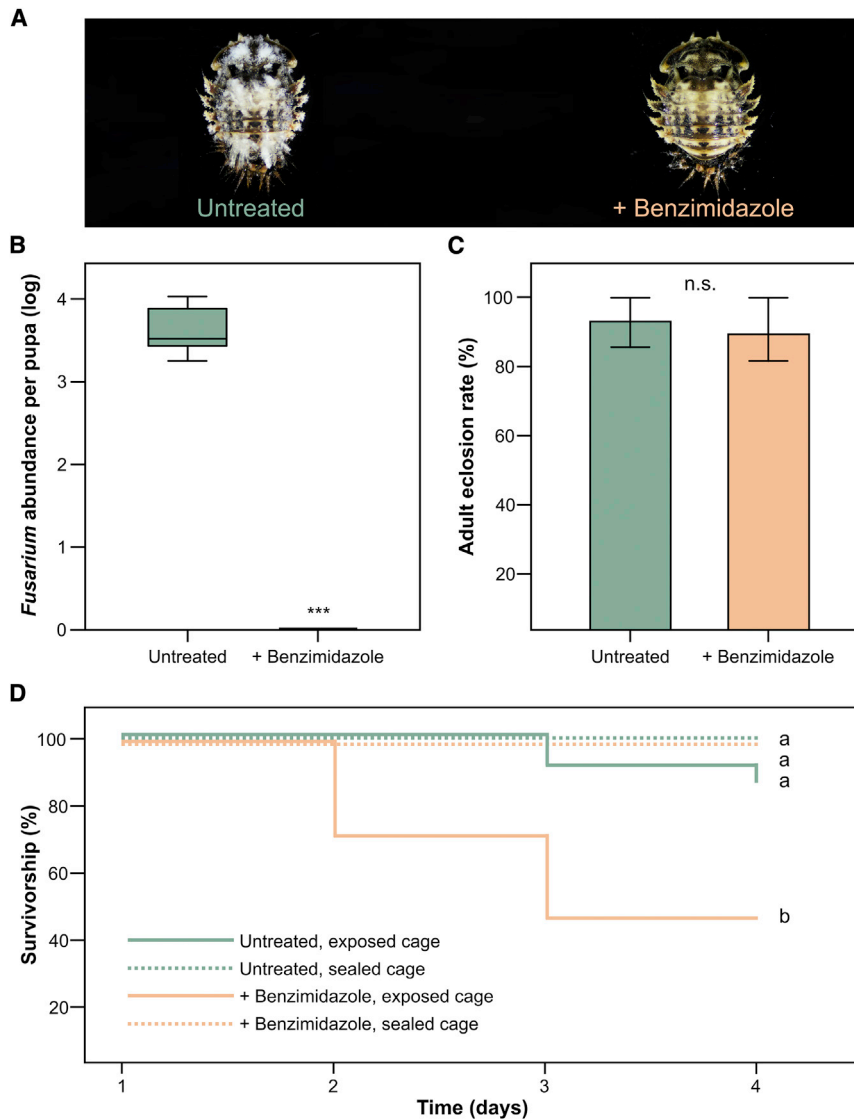


**Figure 3. Symbiont-mediated pupal protection**

(A) Topical application of benzimidazole clears *F. oxysporum* from the outer surfaces of pupae. (B) Symbiont abundance following the quantification of Tef-1  $\alpha$  gene copy numbers ( $n = 16$ ; unpaired Wilcoxon rank-sum test,  $W = 2$ ,  $p = 0.001$ ). Box coloration signifies the experimental treatment. Lines represent medians, boxes comprise the 25–75 percentiles, and whiskers denote the range. Asterisks indicate significant differences.

(C) Adult eclosion rate following benzimidazole treatment ( $n = 46$ ; GLM [binomial],  $\chi^2 = 0$ ,  $df = 1$ ,  $p = 1$ ). Bar coloration signifies the experimental treatment. Whiskers denote the 95% binomial confidence intervals.

(D) Pupal survivorship across treatments ( $n = 98$ ; log-rank test,  $\chi^2 = 34.8$ ,  $df = 3$ ; Cox's model,  $p < 0.001$ , related to [Data S1](#)). Line coloration and patterning signifies the experimental treatment. Letters indicate significant differences between treatments. n.s., not significant.

See also [Video S1](#).

a diversity of host plants, including fig<sup>67</sup> and avocado trees.<sup>68</sup> *Fusarium* may additionally alter insect behavior to promote its propagation as demonstrated in the mealworm beetle (Coleoptera:Tenebrionidae),<sup>69</sup> which preferentially consumes grains colonized by the fungus and continues to produce spore-bearing feces weeks following dietary exposure.<sup>69</sup> As mealworms additionally transmit *Fusarium* to uninfected mates during copulation, the fungus appears to maximize its range by aligning its transmission to the behavioral, reproductive, and nutritional ecology of its host.<sup>69</sup>

As *F. oxysporum* causes wilt disease in a number of plant groups,<sup>59</sup> we additionally examined whether the lineage associated with *C. alternans* induces a pathogenic phenotype upon infecting the sweet potato plant, *I. batatas*. Although *F. oxysporum* infection in plant roots can be asymptomatic, its colonization of vascular tissue triggers massive wilting, necrosis, and chlorosis of leaves and stems.<sup>59,70</sup> By inoculating  $5 \times 10^4$  *F. oxysporum* spores onto the leaf surfaces of *I. batatas*, we observe that the fungus consistently induces

wilt disease (Figure 5A, Pearson's  $\chi^2$  test,  $\chi^2 = 5.32$ ,  $df = 1$ ,  $p = 0.02$ ), which results in a greater proportion of non-viable cells relative to uninfected plants (Figure 5B). As these lesions are characteristic of necrotrophic activity,<sup>71</sup> our findings indicate that *F. oxysporum* retained its plant pathogenic potential in light of its association with tortoise beetles. Given the ubiquity of *Fusarium* lineages in the soil and in association plants, it is conceivable that *F. oxysporum* is acquired by the beetle from the environment every generation and that the benefits to the microbe are negligible relative pupal defense in the insect. Elucidating the transmission route of *F. oxysporum*,

and whether it can consistently propagate in the absence of its beetle host, will determine the degree by which the fungus is simply coopted by *C. alternans*.

### Chromosome-scale symbiont genome assembly and annotation

We sequenced the genome of *F. oxysporum* to characterize its metabolic potential and gain insights into its dual lifestyle as a defensive insect symbiont and plant pathogen. High fidelity (HiFi) sequencing from Pacific Biosciences yielded 148,258 filtered reads with an average length of 13.7 kb. These were assembled into 12 unitigs, or high-quality contigs, representing a haploid genome of 48.6 Mb, with a GC content of 46% and a N50 of 28.5 Mb (Figure 6A). Most unitigs are enriched for telomeric repeats at their edges. Stretches of TTAGGG hexamers were identified at both ends of 10 unitigs, resulting in gapless, telomere-to-telomere assemblies of complete chromosomes, whereas the two remaining unitigs possessed only one telomeric repeat at one end. This indicates that the *F. oxysporum* genome

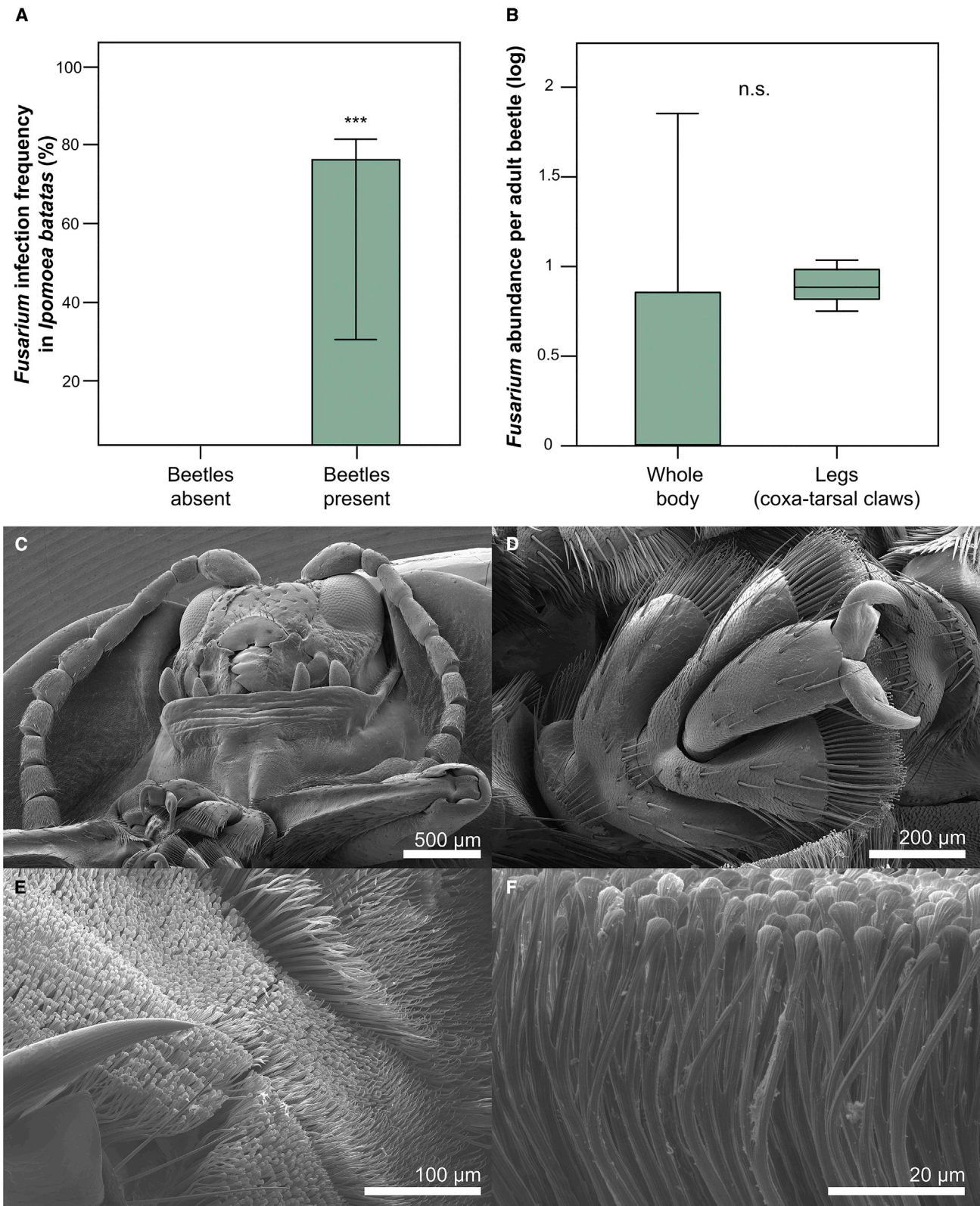


**Figure 4. Tortoise beetles propagate *Fusarium oxysporum* to uninfected host plants**

(A) *F. oxysporum* infection frequencies in the sweet potato plant (*Ipomoea batatas*) grown in the presence and absence of *Chelymorpha alternans* (n = 20; Pearson's  $\chi^2$  test,  $\chi^2 = 5.95$ , df = 1, p = 0.01). Whiskers denote the 95% binomial confidence intervals.

(legend continued on next page)

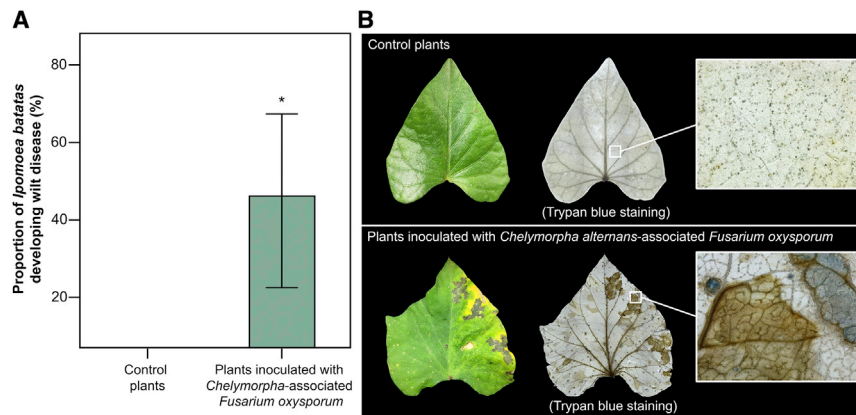


**Figure 5. Pathogenic impact of *Chelymorpha*-associated *Fusarium oxysporum* on the sweet potato plant (*Ipomoea batatas*)**

(A) Plants inoculated with symbiotic *F. oxysporum* from *in vitro* cultures exhibit wilting and yellowing leaves in contrast to the control group ( $n = 27$ ; Pearson's  $\chi^2$  test,  $\chi^2 = 5.32$ ,  $df = 1$ ,  $p = 0.02$ ). Whiskers denote the 95% binomial confidence intervals. Asterisk indicates significant differences. (B) Trypan blue staining of untreated and *F. oxysporum*-inoculated leaves. Coloration distinguishes viable (clear) from non-viable (blue) cells.

is organized into 11–12 chromosomes (Figure 6A). The genome assembly is highly complete with 98.6% of the Benchmarking Universal Single-Copy Orthologs (BUSCO) genes represented against the Ascomycota database. A total of 97.4% of these genes are single copy, 1.1% are duplicated, 0.2% are fragmented, and 1.3% are missing.

The genomes of plant pathogenic oomycetes and fungi display tight physical associations between transposable elements (TE) and genes encoding virulence factors that aid in host colonization and evasion of the immune system.<sup>72,73</sup> These include effector molecules that are regulated through chromatin modification during infection alongside flanking TEs.<sup>57,73</sup> Only 7% of the beetle-associated *F. oxysporum* genome is composed of repetitive sequences, including TEs such as long terminal repeats (3.02%) and DNA transposons (2.52%). In contrast, an estimated 28% of the genome of *F. oxysporum* f.sp. *lycopersici*,<sup>74</sup> a tomato plant pathogen, is composed of repetitive sequences, similar to close relatives that are causal to wilt disease.<sup>57</sup> As TE proliferation is typically tied to genome expansion,<sup>72</sup> we note that the relatively small number of repetitive elements encoded by the fungal symbiont of *C. alternans* correlates to one of the smallest genomes assembled to date for a member of the *F. oxysporum* species complex (Figure 6B), alongside the human-associated strain NRRL 26365.<sup>75</sup> The 10 largest genomes (56–68 Mb) in our analysis all stem from plant pathogens.

Gene prediction and annotation using Funannotate (v.1.8)<sup>76</sup> resulted in 16,925 gene models. The proportion of genes assigned a functional annotation is 50.7%, consistent with recent sequencing efforts for *Fusarium* and other filamentous fungi.<sup>74,77</sup> Most genes assigned a functional classification were categorized under carbohydrate transport and metabolism, followed by secondary metabolite biosynthesis, amino acid metabolism, and posttranslational modification (Figure 6C; Data S2). In contrast, genes involved in cellular motility and extracellular structures were poorly represented (Figure 6C; Data S2).

As fungi are assimilative heterotrophs, enzymes involved in releasing and transporting carbohydrates and extracellular nutrients are critical for their metabolism. Genes encoding hydrolytic enzymes are typically enriched in the genomes of plant pathogenic fungi,<sup>57,73,77</sup> likely facilitating the deconstruction, digestion, and assimilation of the recalcitrant polysaccharides encountered during colonization of the plant cell.<sup>78</sup> We performed a search for carbohydrate-active enzymes (CAZymes) using the dbCAN database.<sup>79</sup> A total of 768 CAZymes were predicted for the fungal symbiont of *C. alternans*, which included 360 glycoside hydrolases (GHs), 125 carbohydrate esterases (CEs), 120 auxiliary activities (AAs), 29 carbohydrate-binding modules (CBMs), and 25 polysaccharide lyases (PLs) (Data S3). These enzymes are predicted to act on most plant cell wall polysaccharides, including cellulose (e.g., GH5 and 9), hemicellulose (e.g., GH43), pectin (e.g., GH28, PL4), and lignin (e.g., AA1, 2 and 5). As a microbe's arsenal of hydrolytic enzymes is strongly correlated with its ecology,<sup>79</sup> we applied the CAZyme-Assisted Training And Sorting of trophicity (CATASTrophy) prediction tool<sup>80</sup> to infer the trophic affiliation and pathogenic potential of *C. alternans*-associated *F. oxysporum*. Trophic predictions following a multivariate analysis classified the symbiont as a vasculartroph (Data S3) that likely alternates between biotrophic and necrotrophic phases, consistent with the assignments of wilt- and rot-causing lineages of the *F. oxysporum* species complex.<sup>80</sup>

The extensive presence of genes encoding plant cell wall-degrading enzymes within the genome of *F. oxysporum* complements the range of basic plant pathogenicity factors annotated in other fusaria,<sup>57</sup> including Ras proteins, G protein-signaling components, and cAMP pathways (Data S4). Most of these pathways encode cellular signaling components that underlie exogenous and endogenous perception and interaction with the host plant. Collectively, our annotation revealed that the fungal symbiont of *C. alternans* possesses many of the molecular signatures tied to a phytopathogenic lifestyle in *F. oxysporum*, reflecting its capacity to infect and colonize the sweet potato plant, *I. batatas* (Figures 4 and 5).

(B) *F. oxysporum* abundance in enclosing beetles following the quantification of Tef-1 $\alpha$  gene copy numbers in legs (spanning the coxa to the tarsal claws) relative to the whole insect ( $n = 6$ ; LM,  $F_{1,4} = 0.48$ ,  $p = 0.53$ ). Lines represent medians, boxes comprise the 25–75 percentiles, and whiskers denote the range. n.s., not significant.

(C–F) Scanning electron microscopy images of (C) a recently enclosed beetle, (D and E) its tarsal claws and pads, and (F) microbe-bearing setae. Scale bars are included for reference.



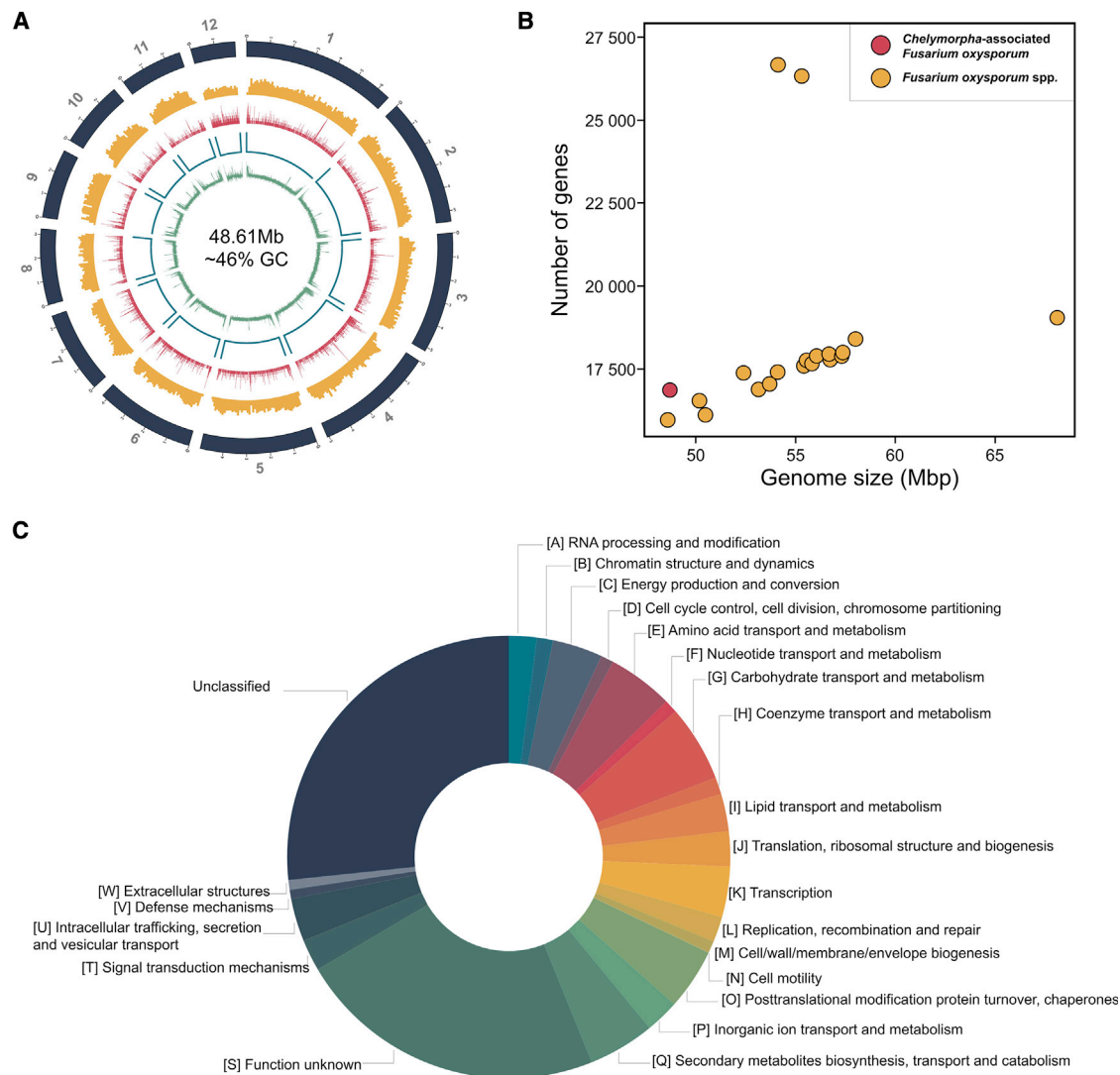


**Figure 6. Genomic features and annotation of *Chelymorpha alternans*-associated *Fusarium oxysporum***

(A) Circular view of the *F. oxysporum* genome. The plot consists of five tracks from the outside: (i) 12 contigs representing the haploid genome, (ii) gene density within 100-kb windows, (iii) repeat count within 1,000 bp windows, (iv) telomeric repeats, and (v) GC content within 1,000 bp windows.

(B) Relationship between genome size and gene content for representative members of the *F. oxysporum* species complex (yellow) relative to the symbiotic lineage associated with *C. alternans* (red).

(C) Functional classification of protein-coding genes according to COG (Clusters of Orthologous Genes) metabolic categories.

See also [Data S2](#), [S4](#), and [S5](#).

### Insecticidal potential of *Fusarium oxysporum*

*Fusarium* species produce a wide variety of secondary metabolites that are toxic to plants and animals,<sup>81</sup> including invertebrates.<sup>82</sup> To explore the metabolic potential of *F. oxysporum* in the defensive biochemistry of *C. alternans* pupae, we surveyed the symbiont's genome assembly for biosynthetic gene clusters using fungiSMASH.<sup>83</sup> For most fungi, secondary metabolites are synthesized by nonribosomal peptide synthetases, polyketide synthases, or terpene synthases.<sup>84</sup> Backbone enzymes encoded in a pathway are flanked by cluster-specific transporters and transcription factors.<sup>57,84</sup> In total, 42 biosynthetic gene clusters were predicted in the symbiont's genome, including 22 non-ribosomal peptides (NRPs), 11 terpenes synthases (TSs), five

polyketide synthases (PKSs), two betalactones, and two indoles (Figure 7A). The majority of these clusters (39) are shared with other fusaria (Figure 7A). However, fusarubin, a polyketide phytotoxin<sup>85</sup>—present in all examined members of the *F. oxysporum* species complex—is not encoded by the defensive symbiont of *C. alternans* (Figure 7A).

We observe that biosynthetic gene clusters are distributed across most, but not all, chromosomes of the symbiont genome. Notably, chromosome 12 lacked any pathways involved in secondary metabolism biosynthesis, possibly reflecting the compartmentalization described in many *Fusarium* genomes.<sup>74</sup> Genomic regions are typically divided into accessory components that encode virulence factors and

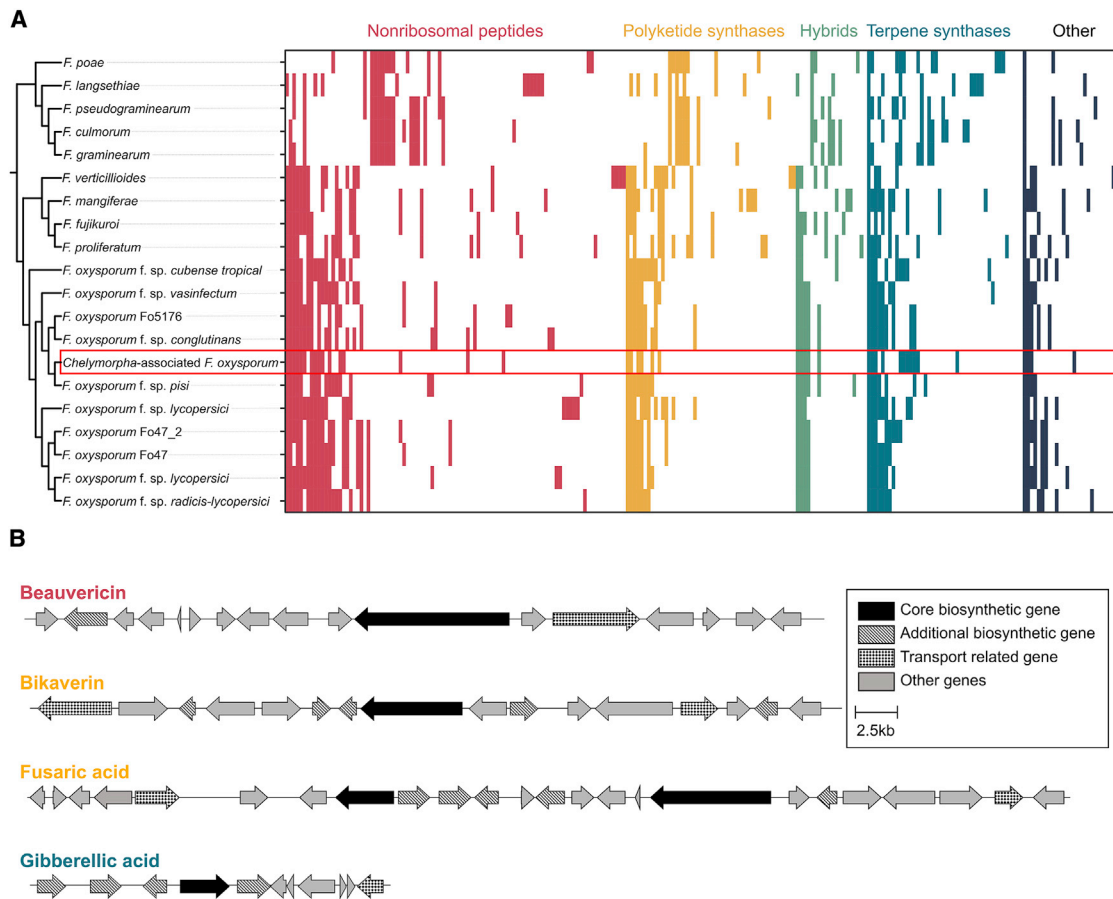


**Figure 7. Secondary metabolism and insecticidal potential of *Chelymormpha*-associated *Fusarium oxysporum***

(A) Heatmap depicting gene cluster family distribution across members of the *F. oxysporum* species complex and closely related fusaria. Each column represents a pathway. Colors indicate the absence, in white, or the presence of BGC classes: red, nonribosomal peptides (NRPS); yellow, polyketide synthases (PKS, including both types I and III); green, NRPS-PKS hybrids; others (including betalactones and indoles). Each row represents a *Fusarium* genome. The depicted dendrogram is an abridged version, related to [Data S5](#), limited to fusarial species.

(B) Predicted biosynthetic gene clusters with potential insecticidal activity in the genome of *Chelymormpha alternans*-associated *Fusarium oxysporum*. Arrow patterns represent different gene functions. Scale bars are included for reference.

biosynthetic gene clusters or core regions that encode functions necessary for growth and survival.<sup>57,74</sup> Indeed, the highest proportion of genes assigned an annotation in chromosome 12 are dedicated to informational processing, including replication and recombination (7.6%), followed by transcription (5.9%) and carbohydrate transport and metabolism (3.9%) ([Data S2](#)).

Of the mycotoxins produced by *Fusarium*, several are known for their insecticidal properties, including beauvericin, gibberellic acid, bikaverin, and fusaric acid.<sup>57,82,86,87</sup> All four encoding biosynthetic gene clusters are retained by *F. oxysporum* in its symbiosis with tortoise beetles ([Figure 7B](#)). Beauvericin, a cyclic antibiotic belonging to the enniatin family, is especially notable given its strong cytotoxic effects against a broad range of insect orders.<sup>86,87</sup> Gibberellic acid, a diterpenoid that induces epithelial degeneration in insects,<sup>88</sup> additionally exhibits potent antifeedant properties that may confer pupal protection in *C. alternans*. This includes repelling insects prior to contact, suppressing biting after contact, and

detering further feeding following consumption.<sup>89,90</sup> By capitalizing on the cultivability of *F. oxysporum*, future efforts will explore the structure and mode of action of the symbiont's secondary metabolites. These will feature targeted approaches that combine mass spectrometry<sup>91</sup> with bioassays in the laboratory and field. If microbe-mediated protection does indeed stem from the production of bioactive compounds, our efforts will additionally elucidate how *C. alternans* withstands the possible inhibitory effects of its mutualist. In rove beetles, increased tolerance against a symbiont's defensive compounds underlies how the host contends with the toxicity of pederin while benefiting from its protective properties against predacious ants.<sup>23</sup> Interestingly, beetles are generally less susceptible to entomopathogenic fusaria relative to other insect orders.<sup>82</sup> Although speculative, a higher tolerance to *Fusarium* and their mycotoxins may have predisposed coleopterans to engage in stable, yet functionally divergent symbioses with members of the fungal genus.<sup>67,91,92,93</sup>

## Conclusions

Pupae counter antagonistic challenges through a remarkable set of defensive adaptations.<sup>35</sup> Here, we highlight the role of symbiosis in upgrading pupal defense for a leaf beetle in exchange for propagating its mutualist. Where plants are increasingly recognized as reservoirs for symbiont infection across several herbivorous insect clades,<sup>94–97</sup> we aim to examine the role of mixed-mode transmission<sup>98</sup> for the persistence of *F. oxysporum* in *C. alternans* populations. Mixed-mode transmission is critical for the epidemiology of numerous symbionts,<sup>98</sup> extending the range of infection strategies available for a microbe to access its host, as demonstrated in firebugs,<sup>99</sup> bees,<sup>100</sup> and wasps.<sup>101</sup> It is conceivable that tortoise beetles acquire their protective symbiont both vertically through maternal endowments (e.g., Kaiwa et al.,<sup>102</sup> Hosokawa et al.,<sup>103</sup> and Pons et al.<sup>104</sup>) and horizontally by consuming infected plants (e.g., Caspi-Fluger et al.<sup>105</sup>). Future efforts will shed light on the ubiquity, specificity, and metabolic conservation of the *Fusarium* symbiosis with the Cassidinae, a highly speciose clade of herbivorous beetles.

## STAR★METHODS

Detailed methods are provided in the online version of this paper and include the following:

- KEY RESOURCES TABLE
- RESOURCE AVAILABILITY
  - Lead contact
  - Materials availability
  - Data and code availability
- EXPERIMENTAL MODEL AND SUBJECT DETAILS
  - Insect rearing
  - Plant rearing
  - Microbial strain maintenance
- METHOD DETAILS
  - Scanning electron microscopy
  - Metagenome sequencing, assembly, and taxonomic assignment
  - Isolation of *Chelymorpha alternans*-associated *Fusarium oxysporum*
  - Diagnostic PCR screening
  - Quantitative PCR
  - Symbiont genome sequencing, assembly, and annotation
  - Phylogenetic reconstruction
  - Symbiont manipulation and survival assays
  - Phytopathogenicity of *F. oxysporum*
- QUANTIFICATION AND STATISTICAL ANALYSIS

## SUPPLEMENTAL INFORMATION

Supplemental information can be found online at <https://doi.org/10.1016/j.cub.2022.07.065>

## ACKNOWLEDGMENTS

We thank Vincensius Oetama and Wilhelm Boland for their insightful discussions and suggestions, Christian Feldhaus (Light Microscopy Facility, Max Planck Institute for Biology) for technical support, Christine Henzler and Alejandra Leyva for their assistance in caring for the beetles, and Ralf Sommer

for helpful comments on a previous version of the manuscript. Julie Johnson (Life Sciences Studios) illustrated Figure 1A. Financial support from the Max Planck Society, the German Research Foundation (EXC2124–390838134, project 09.030 and project BE 6922/1-1), and the Alexander Von Humboldt Foundation is gratefully acknowledged.

## AUTHOR CONTRIBUTIONS

A.B., N.B., and H.S. conceived of the study. A.B., N.B., D.W., K.H., N.Z., and H.S. designed the experiments. N.B., A.B., D.W., M.G.-L., I.P., C.L., V.R., B.S., and H.S. carried out experiments, sequencing work, and analysis. A.B. and H.S. wrote the manuscript. All authors edited and commented on the paper.

## DECLARATION OF INTERESTS

The authors declare no competing interests.

## INCLUSION AND DIVERSITY

We worked to ensure sex balance in the selection of non-human subjects. One or more of the authors of this paper self-identifies as an underrepresented ethnic minority in science. The author list of this paper includes contributors from the location where the research was conducted who participated in the data collection, design, analysis, and/or interpretation of the work.

Received: June 21, 2022

Revised: July 21, 2022

Accepted: July 22, 2022

Published: August 19, 2022

## REFERENCES

1. Hembry, D.H., and Weber, M.G. (2020). Ecological interactions and macroevolution: a new field with old roots. *Annu. Rev. Ecol. Evol. Syst.* 51, 215–243.
2. Paterson, S., Vogwill, T., Buckling, A., Benmayor, R., Spiers, A.J., Thomson, N.R., Quail, M., Smith, F., Walker, D., Libberton, B., et al. (2010). Antagonistic coevolution accelerates molecular evolution. *Nature* 464, 275–278.
3. Brockhurst, M.A., Chapman, T., King, K.C., Mank, J.E., Paterson, S., and Hurst, G.D.D. (2014). Running with the Red Queen: the role of biotic conflicts in evolution. *Proc. Biol. Sci.* 281, 20141382.
4. Betts, A., Gray, C., Zelek, M., MacLean, R.C., and King, K.C. (2018). High parasite diversity accelerates host adaptation and diversification. *Science* 360, 907–911.
5. Flórez, L.V., Biedermann, P.H.W., Engl, T., and Kaltenpoth, M. (2015). Defensive symbioses of animals with prokaryotic and eukaryotic microorganisms. *Nat. Prod. Rep.* 32, 904–936.
6. Koch, H., and Schmid-Hempel, P. (2011). Socially transmitted gut microbiota protect bumble bees against an intestinal parasite. *Proc. Natl. Acad. Sci. USA* 108, 19288–19292.
7. Mendiola, S.Y., Stoy, K.S., DiSalvo, S., Wynn, C.L., Civitello, D.J., and Gerardo, N.M. (2022). Competitive exclusion of phytopathogenic *Serratia marcescens* from squash bug vectors by the gut endosymbiont *Caballeronia*. *Appl. Environ. Microbiol.* 88, e0155021.
8. Pan, X., Zhou, G., Wu, J., Bian, G., Lu, P., Raikhel, A.S., and Xi, Z. (2012). *Wolbachia* induces reactive oxygen species (ROS)-dependent activation of the Toll pathway to control dengue virus in the mosquito *Aedes aegypti*. *Proc. Natl. Acad. Sci. USA* 109, E23–E31.
9. Horak, R.D., Leonard, S.P., and Moran, N.A. (2020). Symbionts shape host innate immunity in honeybees. *Proc. Biol. Sci.* 287, 20201184.
10. Kroiss, J., Kaltenpoth, M., Schneider, B., Schwinger, M.G., Hertweck, C., Maddula, R.K., Strohm, E., and Svatos, A. (2010). Symbiotic *Streptomyces* provide antibiotic combination prophylaxis for wasp offspring. *Nat. Chem. Biol.* 6, 261–263.

- Oh, D.C., Poulsen, M., Currie, C.R., and Clardy, J. (2009). Dentigerumycin: a bacterial mediator of an ant-fungus symbiosis. *Nat. Chem. Biol.* 5, 391–393.
- Bennett, G.M., and Moran, N.A. (2015). Heritable symbiosis: the advantages and perils of an evolutionary rabbit hole. *Proc. Natl. Acad. Sci. USA* 112, 10169–10176.
- Perreau, J., and Moran, N.A. (2022). Genetic innovations in animal-microbe symbioses. *Nat. Rev. Genet.* 23, 23–39.
- Currie, C.R., Wong, B., Stuart, A.E., Schultz, T.R., Rehner, S.A., Mueller, U.G., Sung, G.H., Spatafora, J.W., and Straus, N.A. (2003). Ancient tripartite coevolution in the attine ant-microbe symbiosis. *Science* 299, 386–388.
- Kaltenpoth, M., Roeser-Mueller, K., Koehler, S., Peterson, A., Nechitaylo, T.Y., Stubblefield, J.W., Herzner, G., Seger, J., and Strohm, E. (2014). Partner choice and fidelity stabilize coevolution in a Cretaceous-age defensive symbiosis. *Proc. Natl. Acad. Sci. USA* 111, 6359–6364.
- Nakabachi, A., Ueoka, R., Oshima, K., Teta, R., Mangoni, A., Gurgui, M., Oldham, N.J., van Echten-Deckert, G., Okamura, K., Yamamoto, K., et al. (2013). Defensive bacteriome symbiont with a drastically reduced genome. *Curr. Biol.* 23, 1478–1484.
- King, K.C. (2019). Defensive symbionts. *Curr. Biol.* 29, R78–R80.
- Fenton, A., Johnson, K.N., Brownlie, J.C., and Hurst, G.D.D. (2011). Solving the *Wolbachia* paradox: modeling the tripartite interaction between host, *Wolbachia*, and a natural enemy. *Am. Nat.* 178, 333–342.
- Kloock, A., Bonsall, M.B., and King, K.C. (2020). Evolution and maintenance of microbe-mediated protection under occasional pathogen infection. *Ecol. Evol.* 10, 8634–8642.
- Oliver, K.M., Campos, J., Moran, N.A., and Hunter, M.S. (2008). Population dynamics of defensive symbionts in aphids. *Proc. Biol. Sci.* 275, 293–299.
- Vorburger, C. (2022). Defensive symbionts and the evolution of parasitoid host specialization. *Annu. Rev. Entomol.* 67, 329–346.
- Flórez, L.V., Scherlach, K., Gaube, P., Ross, C., Sitte, E., Hermes, C., Rodrigues, A., Hertweck, C., and Kaltenpoth, M. (2017). Antibiotic-producing symbionts dynamically transition between plant pathogenicity and insect-defensive mutualism. *Nat. Commun.* 8, 15172.
- Kellner, R.L.L., and Dettner, K. (1996). Differential efficacy of toxic pederin in deterring potential arthropod predators of *Paederus* (Coleoptera: Staphylinidae) offspring. *Oecologia* 107, 293–300.
- Kaltenpoth, M., Götter, W., Herzner, G., and Strohm, E. (2005). Symbiotic bacteria protect wasp larvae from fungal infestation. *Curr. Biol.* 15, 475–479.
- Oliver, K.M., Degnan, P.H., Hunter, M.S., and Moran, N.A. (2009). Bacteriophages encode factors required for protection in a symbiotic mutualism. *Science* 325, 992–994.
- Hammer, T.J., and Moran, N.A. (2019). Links between metamorphosis and symbiosis in holometabolous insects. *Philos. Trans. R. Soc. Lond. B Biol. Sci.* 374, 20190068.
- Elkinton, J.S., and Liebhold, A.M. (1990). Population dynamics of gypsy moth in North America. *Annu. Rev. Entomol.* 35, 571–596.
- Hanski, I., and Parviainen, P. (1985). Cocoon predation by small mammals, and pine sawfly population dynamics. *Oikos* 45, 125–136.
- East, R. (1974). Predation on the soil-dwelling stages of the winter moth at Wytham woods, Berkshire. *J. Anim. Ecol.* 43, 611.
- Heisswolf, A., Klemola, N., Ammúnét, T., and Klemola, T. (2009). Responses of generalist invertebrate predators to pupal densities of autumnal and winter moths under field conditions. *Ecol. Entomol.* 34, 709–717.
- Mappes, J., Kokko, H., Ojala, K., and Lindström, L. (2014). Seasonal changes in predator community switch the direction of selection for prey defences. *Nat. Commun.* 5, 5016.
- Murphy, S.M., and Lill, J.T. (2010). Winter predation of diapausing cocoons of slug caterpillars (Lepidoptera: Limacodidae). *Environ. Entomol.* 39, 1893–1902.
- Battisti, A., Bernardi, M., and Ghiraldo, C. (2000). Predation by the hoopee (*Upupa epops*) on pupae of *Thaumetopoea pityocampa* and the likely influence on other natural enemies. *BioControl* 45, 311–323.
- Kollberg, I., Bylund, H., Huitu, O., and Björkman, C. (2014). Regulation of forest defoliating insects through small mammal predation: reconsidering the mechanisms. *Oecologia* 176, 975–983.
- Lindstedt, C., Murphy, L., and Mappes, J. (2019). Antipredator strategies of pupae: how to avoid predation in an immobile life stage? *Philos. Trans. R. Soc. Lond. B Biol. Sci.* 374, 20190069.
- Ruxton, G.D., Sherratt, T.N., and Speed, M.P. (2004). *Avoiding Attack: The Evolutionary Ecology of Crypsis, Warning Signals and Mimicry* (OUP Oxford).
- Craig, C.L. (1997). Evolution of arthropod silks. *Annu. Rev. Entomol.* 42, 231–267.
- Sugiura, S., and Yamazaki, K. (2014). Caterpillar hair as a physical barrier against invertebrate predators. *Behav. Ecol.* 25, 975–983.
- Deyrup, S.T., Eckman, L.E., Lucadamo, E.E., McCarthy, P.H., Knapp, J.C., and Smedley, S.R. (2014). Antipredator activity and endogenous biosynthesis of defensive secretion in larval and pupal *Delphastus catalinae* (Horn) (Coleoptera: Coccinellidae). *Chemoecology* 24, 145–157.
- Chaboo, C.S. (2007). Biology and phylogeny of the Cassidinae Gyllenhal sensu lato (tortoise and leaf-mining beetles) (Coleoptera: Chrysomelidae). *Bull. Am. Museum Nat. Hist.* 305, 1–250.
- Salem, H., Kirsch, R., Pauchet, Y., Berasategui, A., Fukumori, K., Moriyama, M., Cripps, M., Windsor, D., Fukatsu, T., and Gerardo, N.M. (2020). Symbiont digestive range reflects host plant breadth in herbivorous beetles. *Curr. Biol.* 30, 2875–2886.e4.
- Bauer, E., Kaltenpoth, M., and Salem, H. (2020). Minimal fermentative metabolism fuels extracellular symbiont in a leaf beetle. *ISME J.* 14, 866–870.
- Salem, H., Bauer, E., Kirsch, R., Berasategui, A., Cripps, M., Weiss, B., Koga, R., Fukumori, K., Vogel, H., Fukatsu, T., and Kaltenpoth, P. (2017). Drastic genome reduction in an herbivore's pectinolytic symbiont. *Cell* 171, 1520–1531.e13.
- Keller, G.P., Windsor, D.M., Saucedo, J.M., and Werren, J.H. (2004). Reproductive effects and geographical distributions of two *Wolbachia* strains infecting the Neotropical beetle, *Chelymormpha alternans* Boh. (Chrysomelidae, Cassidinae). *Mol. Ecol.* 13, 2405–2420.
- Morrison, C.R., and Windsor, D.M. (2018). The life history of *Chelymormpha alternans* (Coleoptera: Chrysomelidae: Cassidinae) in Panamá. *Ann. Entomol. Soc. Am.* 111, 31–41.
- Gruber-Vodicka, H.R., Seah, B.K.B., and Pruesse, E. (2020). phyloFlash: rapid small-subunit rRNA profiling and targeted assembly from metagenomes. *mSystems* 5, e00920.
- Venci, F.V., and Srygley, R.B. (2013). Enemy targeting, trade-offs, and the evolutionary assembly of a tortoise beetle defense arsenal. *Evol. Ecol.* 27, 237–252.
- Windsor, D.M. (1987). Natural history of a subsocial tortoise beetle, *Acromis Sparsa Boheman* (Chrysomelidae, Cassidinae) in Panama. *Psyche* 94, 127–150.
- Zhou, Y., Xu, J., Zhu, Y., Duan, Y., and Zhou, M. (2016). Mechanism of action of the benzimidazole fungicide on *Fusarium graminearum*: interfering with polymerization of monomeric tubulin but not polymerized microtubule. *Phytopathology* 106, 807–813.
- Wilson, E.O., and Hölldobler, B. (2005). The rise of the ants: a phylogenetic and ecological explanation. *Proc. Natl. Acad. Sci. USA* 102, 7411–7414.
- Currie, C.R., Scott, J.A., Summerbell, R.C., and Malloch, D. (1999). Fungus-growing ants use antibiotic-producing bacteria to control garden parasites. *Nature* 398, 701–704.

52. Scott, J.J., Oh, D.C., Yuceer, M.C., Klepzig, K.D., Clardy, J., and Currie, C.R. (2008). Bacterial protection of beetle-fungus mutualism. *Science* 322, 63.
53. Schmidt, S., Kildgaard, S., Guo, H., Beemelmans, C., and Poulsen, M. (2022). The chemical ecology of the fungus-farming termite symbiosis. *Nat. Prod. Rep.* 39, 231–248.
54. Piel, J., Höfer, I., and Hui, D. (2004). Evidence for a symbiosis island involved in horizontal acquisition of pederin biosynthetic capabilities by the bacterial symbiont of *Paederus fuscipes* beetles. *J. Bacteriol.* 186, 1280–1286.
55. Kellner, R.L.L. (2002). Molecular identification of an endosymbiotic bacterium associated with pederin biosynthesis in *Paederus sabaeus* (Coleoptera: Staphylinidae). *Insect Biochem. Mol. Biol.* 32, 389–395.
56. Piel, J. (2002). A polyketide synthase-peptide synthetase gene cluster from an uncultured bacterial symbiont of *Paederus* beetles. *Proc. Natl. Acad. Sci. USA* 99, 14002–14007.
57. Ma, L.J., Geiser, D.M., Proctor, R.H., Rooney, A.P., O'Donnell, K., Trail, F., Gardiner, D.M., Manners, J.M., and Kazan, K. (2013). *Fusarium* pathogenomics. *Annu. Rev. Microbiol.* 67, 399–416.
58. Summerell, B.A. (2019). Resolving *Fusarium*: current status of the genus. *Annu. Rev. Phytopathol.* 57, 323–339.
59. Gordon, T.R. (2017). *Fusarium oxysporum* and the *Fusarium* Wilt syndrome. *Annu. Rev. Phytopathol.* 55, 23–39.
60. Morrison, C.R., Aubert, C., and Windsor, D.M. (2019). Variation in host plant usage and diet breadth predict sibling preference and performance in the Neotropical tortoise beetle *Chelymormpha alternans* (Coleoptera: Chrysomelidae: Cassidinae). *Environ. Entomol.* 48, 382–394.
61. Wielkopolan, B., Jakubowska, M., and Obrepalska-Stęplowska, A. (2021). Beetles as plant pathogen vectors. *Front. Plant Sci.* 12, 748093.
62. Fox, J.W., Wood, D.L., Koehler, C.S., and O'Keefe, S.T. (1991). Engraver beetles (Scolytidae: *IPS* species) as vectors of the pitch canker fungus, *Fusarium subglutinans*. *Can. Entomol.* 123, 1355–1367.
63. Storer, A.J., Wood, D.L., and Gordon, T.R. (2004). Twig beetles, *Pityophthorus* spp. (Coleoptera: Scolytidae), as vectors of the pitch canker pathogen in California. *Can. Entomol.* 136, 685–693.
64. Salem, H., and Kaltenpoth, M. (2022). Beetle–bacterial symbioses: endless forms most functional. *Annu. Rev. Entomol.* 67, 201–219.
65. McKenna, D.D., Shin, S., Ahrens, D., Balke, M., Beza-Beza, C., Clarke, D.J., Donath, A., Escalona, H.E., Friedrich, F., Letsch, H., et al. (2019). The evolution and genomic basis of beetle diversity. *Proc. Natl. Acad. Sci. USA* 116, 24729–24737.
66. Barraclough, T.G., Barclay, M.V., and Vogler, A.P. (1998). Species richness: does flower power explain beetle-mania? *Curr. Biol.* 8, R843–R845.
67. Jiang, Z.R., Masuya, H., and Kajimura, H. (2021). Novel symbiotic association between *Euwallacea* ambrosia beetle and *Fusarium* fungus on fig trees in Japan. *Front. Microbiol.* 12, 725210.
68. Salman, M., Mahmoud, R., Fadda, Z., Alabdallah, O., Najjar, K., Radwan, J., and Abuamsha, R. (2019). First report of *Fusarium euwallaceae* on avocado trees in Palestine. *Arch. Phytopathol. Plant Prot.* 52, 930–937.
69. Guo, Z., Pfohl, K., Karlovsky, P., Dehne, H.W., and Altincicek, B. (2018). Dissemination of *Fusarium proliferatum* by mealworm beetle *Tenebrio molitor*. *PLoS One* 13, e0204602.
70. Nelson, P.E. (1981). Life cycle and epidemiology of *Fusarium oxysporum*. In *Fungal Wilt Diseases of Plants* (Elsevier), pp. 51–80.
71. Strober, W. (2015). Trypan blue exclusion test of cell viability. *Curr. Protoc. Immunol.* 111, A3.B.1–A3.B.3.
72. Fouché, S., Oggenfuss, U., Chanclud, E., and Croll, D. (2022). A devil's bargain with transposable elements in plant pathogens. *Trends Genet.* 38, 222–230.
73. Sánchez-Vallet, A., Fouché, S., Fudal, I., Hartmann, F.E., Soyer, J.L., Tellier, A., and Croll, D. (2018). The genome biology of effector gene evolution in filamentous plant pathogens. *Annu. Rev. Phytopathol.* 56, 21–40.
74. Ma, L.J., van der Does, H.C., Borkovich, K.A., Coleman, J.J., Daboussi, M.J., Di Pietro, A., Dufresne, M., Freitag, M., Grabherr, M., Henrissat, B., et al. (2010). Comparative genomics reveals mobile pathogenicity chromosomes in *Fusarium*. *Nature* 464, 367–373.
75. O'Donnell, K., Sutton, D.A., Rinaldi, M.G., Magnon, K.C., Cox, P.A., Revankar, S.G., Sanche, S., Geiser, D.M., Juba, J.H., van Burik, J.A., et al. (2004). Genetic diversity of human pathogenic members of the *Fusarium oxysporum* complex inferred from multilocus DNA sequence data and amplified fragment length polymorphism analyses: evidence for the recent dispersion of a geographically widespread clonal lineage and nosocomial origin. *J. Clin. Microbiol.* 42, 5109–5120.
76. Palmer, J.M., and Stajich, J. (2020) Funannotate v1.8.1: Eukaryotic Genome Annotation.
77. Fokkens, L., Guo, L., Dora, S., Wang, B., Ye, K., Sánchez-Rodríguez, C., and Croll, D. (2020). A chromosome-scale genome assembly for the *Fusarium oxysporum* strain Fo5176 to establish a model *Arabidopsis*-fungal pathosystem. *G3 (Bethesda)* 10, 3549–3555.
78. Bradley, E.L., Ökmen, B., Doeblemann, G., Henrissat, B., Bradshaw, R.E., and Mesarich, C.H. (2022). Secreted glycoside hydrolase proteins as effectors and invasion patterns of plant-associated fungi and oomycetes. *Front. Plant Sci.* 13, 853106.
79. Yin, Y., Mao, X., Yang, J., Chen, X., Mao, F., and Xu, Y. (2012). dbCAN: a web resource for automated carbohydrate-active enzyme annotation. *Nucleic Acids Res.* 40, W445–W451.
80. Hane, J.K., Paxman, J., Jones, D.A.B., Oliver, R.P., and de Wit, P. (2019). “CATAStrophy,” a genome-informed trophic classification of filamentous plant pathogens – how many different types of filamentous plant pathogens are there. *Front. Microbiol.* 10, 3088.
81. Nestic, K., Ivanovic, S., and Nestic, V. (2014). Fusarial toxins: secondary metabolites of *Fusarium* fungi. *Rev. Environ. Contam. Toxicol.* 228, 101–120.
82. Teetor-Barsch, G.H., and Roberts, D.W. (1983). Entomogenous *Fusarium* species. *Mycopathologia* 84, 3–16.
83. Medema, M.H., Blin, K., Cimermancic, P., de Jager, V., Zakrzewski, P., Fischbach, M.A., Weber, T., Takano, E., and Breitling, R. (2011). antiSMASH: rapid identification, annotation and analysis of secondary metabolite biosynthesis gene clusters in bacterial and fungal genome sequences. *Nucleic Acids Res.* 39, W339–W346.
84. Keller, N.P. (2019). Fungal secondary metabolism: regulation, function and drug discovery. *Nat. Rev. Microbiol.* 17, 167–180.
85. Gopalakrishnan, S., Beale, M.H., Ward, J.L., and Strange, R.N. (2005). Chickpea wilt: identification and toxicity of 8-O-methyl-fusarubin from *Fusarium acutatum*. *Phytochemistry* 66, 1536–1539.
86. Grove, J.F., and Pople, M. (1980). The insecticidal activity of beauvericin and the enniatin complex. *Mycopathologia* 70, 103–105.
87. Wang, Q., and Xu, L. (2012). Beauvericin, a bioactive compound produced by fungi: a short review. *Molecules* 17, 2367–2377.
88. Abboud, M.A.A. (2014). Bioimpact of application of pesticides with plant growth hormone (gibberellic acid) on target and non-target microorganisms. *J. Saudi Chem. Soc.* 18, 1005–1010.
89. Abdellaoui, K., Halima-Kamel, M.B., and Ben, M.H. (2009). The antifeeding and repellent properties of gibberellic acid against Asiatic migratory locust *Locusta migratoria*. *Tunis. J. Plant Prot.* 4, 57–66.
90. Shayegan, D., Jalali Sendi, J.J., Sahragard, A., and Zibae, A. (2019). Antifeedant and cytotoxic activity of gibberellic acid against *Helicoverpa armigera* (Hübner) (Lepidoptera: Noctuidae). *Physiol. Entomol.* 44, 169–176.
91. Clevenger, K.D., Bok, J.W., Ye, R., Miley, G.P., Verdán, M.H., Velk, T., Chen, C., Yang, K., Robey, M.T., Gao, P., et al. (2017). A scalable platform to identify fungal secondary metabolites and their gene clusters. *Nat. Chem. Biol.* 13, 895–901.
92. Freeman, S., Sharon, M., Maymon, M., Mendel, Z., Protasov, A., Aoki, T., Eskalen, A., and O'Donnell, K. (2013). *Fusarium euwallaceae* sp. nov.–a

- symbiotic fungus of *Ewallacea* sp., an invasive ambrosia beetle in Israel and California. *Mycologia* 105, 1595–1606.
93. Geib, S.M., Scully, E.D., Jimenez-Gasco, Mdel M., Carlson, J.E., Tien, M., and Hoover, K. (2012). Phylogenetic analysis of *Fusarium solani* associated with the Asian longhorned beetle, *Anoplophora glabripennis*. *Insects* 3, 141–160.
94. Salem, H., Florez, L., Gerardo, N., and Kaltenpoth, M. (2015). An out-of-body experience: the extracellular dimension for the transmission of mutualistic bacteria in insects. *Proc. Biol. Sci.* 282, 20142957.
95. Frago, E., Dicke, M., and Godfray, H.C.J. (2012). Insect symbionts as hidden players in insect–plant interactions. *Trends Ecol. Evol.* 27, 705–711.
96. Chrostek, E., Pelz-Stelinski, K., Hurst, G.D.D., and Hughes, G.L. (2017). Horizontal transmission of intracellular insect symbionts via plants. *Front. Microbiol.* 8, 2237.
97. Pons, I., Renoz, F., Noël, C., and Hance, T. (2019). Circulation of the cultivable symbiont *Serratia symbiotica* in aphids is mediated by plants. *Front. Microbiol.* 10, 764.
98. Ebert, D. (2013). The epidemiology and evolution of symbionts with mixed-mode transmission. *Annu. Rev. Ecol. Evol. Syst.* 44, 623–643.
99. Salem, H., Onchuru, T.O., Bauer, E., and Kaltenpoth, M. (2015). Symbiont transmission entails the risk of parasite infection. *Biol. Lett.* 11, 20150840.
100. Drew, G.C., Budge, G.E., Frost, C.L., Neumann, P., Siozios, S., Yañez, O., and Hurst, G.D.D. (2021). Transitions in symbiosis: evidence for environmental acquisition and social transmission within a clade of heritable symbionts. *ISME J.* 15, 2956–2968.
101. Parratt, S.R., Frost, C.L., Schenkel, M.A., Rice, A., Hurst, G.D.D., and King, K.C. (2016). Superparasitism drives heritable symbiont epidemiology and host sex ratio in a wasp. *PLoS Pathog.* 12, e1005629.
102. Kaiwa, N., Hosokawa, T., Nikoh, N., Tanahashi, M., Moriyama, M., Meng, X.Y., Maeda, T., Yamaguchi, K., Shigenobu, S., Ito, M., and Fukatsu, T. (2014). Symbiont-supplemented maternal investment underpinning host's ecological adaptation. *Curr. Biol.* 24, 2465–2470.
103. Hosokawa, T., Hironaka, M., Mukai, H., Inadomi, K., Suzuki, N., and Fukatsu, T. (2012). Mothers never miss the moment: a fine-tuned mechanism for vertical symbiont transmission in a subsocial insect. *Anim. Behav.* 83, 293–300.
104. Pons, I., González Porras, M.Á., Breitenbach, N., Berger, J., Hipp, K., and Salem, H. (2022). For the road: calibrated maternal investment in light of extracellular symbiont transmission. *Proc. Biol. Sci.* 289, 20220386.
105. Caspi-Fluger, A., Inbar, M., Mozes-Daube, N., Katzir, N., Portnoy, V., Belausov, E., Hunter, M.S., and Zchori-Fein, E. (2012). Horizontal transmission of the insect symbiont *Rickettsia* is plant-mediated. *Proc. Biol. Sci.* 279, 1791–1796.
106. Zarrin, M., Ganj, F., and Faramarzi, S. (2016). Development of a polymerase chain reaction-restriction fragment length polymorphism method for identification of the *Fusarium* genus using the transcription elongation factor-1 $\alpha$  gene. *Biomed. Rep.* 5, 705–708.
107. Bolger, A.M., Lohse, M., and Usadel, B. (2014). Trimmomatic: a flexible trimmer for Illumina sequence data. *Bioinformatics* 30, 2114–2120.
108. Nurk, S., Meleshko, D., Korobeynikov, A., and Pevzner, P.A. (2017). metaSPAdes: a new versatile metagenomic assembler. *Genome Res.* 27, 824–834.
109. Smit, A.F.A., Hubley, R., and Green, P. (2015) RepeatMasker Open-4.0.
110. Stanke, M., and Morgenstern, B. (2005). Augustus: a web server for gene prediction in eukaryotes that allows user-defined constraints. *Nucleic Acids Res.* 33, W465–W467.
111. Besemer, J., and Borodovsky, M. (2005). GeneMark: web software for gene finding in prokaryotes, eukaryotes and viruses. *Nucleic Acids Res.* 33, W451–W454.
112. Korf, I. (2004). Gene finding in novel genomes. *BMC Bioinformatics* 5, 59.
113. Majoros, W.H., Pertea, M., and Salzberg, S.L. (2004). TigrScan and GlimmerHMM: two open source *ab initio* eukaryotic gene-finders. *Bioinformatics* 20, 2878–2879.
114. Haas, B.J., Salzberg, S.L., Zhu, W., Pertea, M., Allen, J.E., Orvis, J., White, O., Buell, C.R., and Wortman, J.R. (2008). Automated eukaryotic gene structure annotation using EVIDENCEModeler and the program to assemble spliced alignments. *Genome Biol.* 9, R7.
115. Jones, P., Binns, D., Chang, H.Y., Fraser, M., Li, W., McAnulla, C., McWilliam, H., Maslen, J., Mitchell, A., Nuka, G., et al. (2014). InterProScan 5: Genome-scale protein function classification. *Bioinformatics* 30, 1236–1240.
116. Huerta-Cepas, J., Forslund, K., Coelho, L.P., Szklarczyk, D., Jensen, L.J., von Mering, C., and Bork, P. (2017). Fast genome-wide functional annotation through orthology assignment by eggNOG-mapper. *Mol. Biol. Evol.* 34, 2115–2122.
117. Almagro Armenteros, J.J.A., Tsirigos, K.D., Sønderby, C.K., Petersen, T.N., Winther, O., Brunak, S., von Heijne, G., and Nielsen, H. (2019). SignalP 5.0 improves signal peptide predictions using deep neural networks. *Nat. Biotechnol.* 37, 420–423.
118. Käll, L., Krogh, A., and Sonnhammer, E.L.L. (2007). Advantages of combined transmembrane topology and signal peptide prediction—the Phobius web server. *Nucleic Acids Res.* 35, W429–W432.
119. Eddy, S.R. (2011). Accelerated profile HMM Searches. *PLoS Comput. Biol.* 7, e1002195.
120. Zhang, H., Yohe, T., Huang, L., Entwistle, S., Wu, P., Yang, Z., Busk, P.K., Xu, Y., and Yin, Y. (2018). dbCAN2: a meta server for automated carbohydrate-active enzyme annotation. *Nucleic Acids Res.* 46, W95–W101.
121. Blin, K., Shaw, S., Steinke, K., Villebro, R., Ziemert, N., Lee, S.Y., Medema, M.H., and Weber, T. (2019). antiSMASH 5.0: updates to the secondary metabolite genome mining pipeline. *Nucleic Acids Res.* 47, W81–W87.
122. Kanehisa, M., Sato, Y., and Morishima, K. (2016). BlastKOALA and GhostKOALA: KEGG tools for functional characterization of genome and metagenome sequences. *J. Mol. Biol.* 428, 726–731.
123. Seppey, M., Manni, M., and Zdobnov, E.M. (2019). BUSCO: assessing genome assembly and annotation completeness. *Methods Mol. Biol.* 1962, 227–245.
124. Livingstone, P.G., Morphew, R.M., and Whitworth, D.E. (2018). Genome sequencing and pan-genome analysis of 23 *Corallocooccus* spp. strains reveal unexpected diversity, with particular plasticity of predatory gene sets. *Front. Microbiol.* 9, 3187.
125. McGowan, J., O'Hanlon, R., Owens, R.A., and Fitzpatrick, D.A. (2020). Comparative genomic and proteomic analyses of three widespread *Phytophthora* species: *Phytophthora chlamydospora*, *Phytophthora gonapodyides* and *Phytophthora pseudosyringae*. *Microorganisms* 8, 653.
126. McGowan, J., and Fitzpatrick, D.A. (2020). Recent advances in oomycete genomics. *Adv. Genet.* 105, 175–228.
127. Edgar, R.C. (2004). MUSCLE: multiple sequence alignment with high accuracy and high throughput. *Nucleic Acids Res.* 32, 1792–1797.
128. Capella-Gutiérrez, S., Silla-Martínez, J.M., and Gabaldón, T. (2009). trimAl: a tool for automated alignment trimming in large-scale phylogenetic analyses. *Bioinformatics* 25, 1972–1973.
129. Minh, B.Q., Schmidt, H.A., Chernomor, O., Schrempf, D., Woodhams, M.D., von Haeseler, A., and Lanfear, R. (2020). IQ-TREE 2: New models and efficient methods for phylogenetic inference in the genomic era. *Mol. Biol. Evol.* 37, 1530–1534.
130. Letunic, I., and Bork, P. (2021). Interactive Tree Of Life (iTOL) v5: an online tool for phylogenetic tree display and annotation. *Nucleic Acids Res.* 49, W293–W296.
131. R Core Team (2019). R: A language and environment for statistical computing. <http://r.meteo.uni.wroc.pl/web/packages/dPIR/vignettes/intro-dPIR.pdf>.
132. Pathan, E.K., Ghormade, V., and Deshpande, M.V. (2017). Selection of reference genes for quantitative real-time RT-PCR assays in different

- morphological forms of dimorphic zygomycetous fungus *Benjaminiella poitrasii*. *PLoS One* *12*, e0179454.
133. Penouilh-Suzette, C., Fourré, S., Besnard, G., Godiard, L., and Pecrix, Y. (2020). A simple method for high molecular-weight genomic DNA extraction suitable for long-read sequencing from spores of an obligate biotroph oomycete. *J. Microbiol. Methods* *178*, 106054.
134. Palmer, J. (2017). Funannotate: Fungal Genome Annotation Scripts.
135. UniProt Consortium (2019). UniProt: a worldwide hub of protein knowledge. *Nucleic Acids Res.* *47*, D506–D515.
136. Huerta-Cepas, J., Szklarczyk, D., Heller, D., Hernández-Plaza, A., Forslund, S.K., Cook, H., Mende, D.R., Letunic, I., Rattei, T., Jensen, L.J., et al. (2019). eggNOG 5.0: a hierarchical, functionally and phylogenetically annotated orthology resource based on 5090 organisms and 2502 viruses. *Nucleic Acids Res.* *47*, D309–D314.
137. Rawlings, N.D., Barrett, A.J., Thomas, P.D., Huang, X., Bateman, A., and Finn, R.D. (2018). The Merops database of proteolytic enzymes, their substrates and inhibitors in 2017 and a comparison with peptidases in the PANTHER database. *Nucleic Acids Res.* *46*, D624–D632.
138. Urban, M., Cuzick, A., Seager, J., Wood, V., Rutherford, K., Venkatesh, S.Y., De Silva, N., Martinez, M.C., Pedro, H., Yates, A.D., et al. (2020). PHI-base: the pathogen–host interactions database. *Nucleic Acids Res.* *48*, D613–D620.
139. Kalyaanamoorthy, S., Minh, B.Q., Wong, T.K.F., von Haeseler, A., and Jermin, L.S. (2017). ModelFinder: fast model selection for accurate phylogenetic estimates. *Nat. Methods* *14*, 587–589.
140. Mani, B.M. (1994). Systemic acquired resistance in *Arabidopsis thaliana* induced by a predisposing infection with a pathogenic isolate of *Fusarium oxysporum*. *Mol. Plant Microbe Interact.* *7*, 378.
141. Therneau, T.M., and Grambsch, P.M. (2000). *Modeling Survival Data: Extending the Cox Model* (Springer).
142. Wickham, H. (2016). *ggplot2: Elegant Graphics for Data Analysis* (Springer).

**STAR★METHODS**

**KEY RESOURCES TABLE**

REAGENT or RESOURCE	SOURCE	IDENTIFIER
<b>Biological samples</b>		
<i>Chelymorpha alternans</i> maintained at the Max Planck Institute for Biology	This paper	N/A
<i>Ipomoea batatas</i> plants	This paper	N/A
<i>Fusarium oxysporum</i> isolated from <i>Chelymorpha alternans</i>	This paper	N/A
<b>Chemicals, peptides, and recombinant proteins</b>		
Glutaraldehyde	Science Services	Cat#E16220
Osmium tetroxide	Science Services	Cat#E19134
Ethanol	Roth	Cat#9065.2
CO <sub>2</sub>	Air Liquide	I5110S13T0A001
Benzimidazole	Tokio Chemical Industry	Lot. UA7IN-GW
Potato dextrose agar	Merck Millipore	Cat# 1101300500
Potato dextrose broth	VWR chemicals	Cat# SIALP6685
Trypan blue solution	Merck	Cat#T6146
Chloral hydrate	Sigma-Aldrich	Cat#C8383-250G
<b>Critical commercial assays</b>		
QIAGEN DNeasy Blood & Tissue Kit	QIAGEN	Cat#69506
NEBNext Ultra II DNA Library Prep with Sample Purification Beads	New England Biolabs	Cat#E7103S
NEBNext Multiplex Oligos for Illumina (Index Primers Set 1)	New England Biolabs	Cat#E7335S
Qubit dsDNA HS Assay Kit	Thermo Fisher	Cat#Q32854
Agilent High Sensitivity DNA Kit	Agilent	Cat#5067-4626
SMRTbell Express Template Prep Kit 2.0	Pacific Biosciences	Cat#100-938-900
AMPure PB Beads	Pacific Biosciences	Cat#100-265-900
SMRTbell Enzyme Clean Up Kit 2.0	Pacific Biosciences	Cat#101-932-600
Sequencing Primer v5	Pacific Biosciences	Cat#102-067-400
BluePippin System 0.75% Agarose Cassettes, Marker S1	Pacific Biosciences	Cat#BLU0001
Sequel II Binding Kit 2.2	Pacific Biosciences	Cat#101-894-200
Sequel II Sequencing Kit 2.0	Pacific Biosciences	Cat#101-820-200
SMRT Cell 8M Tray	Pacific Biosciences	Cat#101-389-001
DreamTaq Green PCR Master Mix	Thermo Scientific	K1081
Platinum SYBR Green qPCR SuperMix-UDG	Thermo Scientific	Cat#11744100
DNeasy Plant Mini Kit	Qiagen	Cat#69104
<b>Deposited data</b>		
Genome of <i>F. oxysporum</i> associated with <i>C. alternans</i>	This study	GeneBank: SAMN29790836: <a href="https://dataview.ncbi.nlm.nih.gov/object/SAMN29790836">https://dataview.ncbi.nlm.nih.gov/object/SAMN29790836</a>
Metagenome of <i>C. alternans</i> pupae	This study	GeneBank: SAMN29793438: <a href="https://dataview.ncbi.nlm.nih.gov/object/SAMN29793438">https://dataview.ncbi.nlm.nih.gov/object/SAMN29793438</a>
<b>Oligonucleotides</b>		
TEF-Fu3f: GGTATCGACAAGCGAACCAT	Zarrin et al. <sup>106</sup>	<a href="https://www.spandidos-publications.com/10.3892/br.2016.783">https://www.spandidos-publications.com/10.3892/br.2016.783</a>
TEF-Fu3r_2: TAGTAGCGAGGAGTCTCGAA	Zarrin et al. <sup>106</sup>	<a href="https://www.spandidos-publications.com/10.3892/br.2016.783">https://www.spandidos-publications.com/10.3892/br.2016.783</a>

(Continued on next page)



**Continued**

REAGENT or RESOURCE	SOURCE	IDENTIFIER
Software and algorithms		
Trimmomatic v0.03	Bolger et al. <sup>107</sup>	<a href="http://www.usadellab.org/cms/index.php?%20page=trimmomatic">http://www.usadellab.org/cms/index.php?%20page=trimmomatic</a>
SPAdes	Nurk et al. <sup>108</sup>	<a href="https://github.com/ablab/spades">https://github.com/ablab/spades</a>
phyloFlash	Gruber-Vodicka et al. <sup>46</sup>	<a href="http://hrgv.github.io/phyloFlash/">http://hrgv.github.io/phyloFlash/</a>
Funannotate v.1.8.3	Palmer et al. <sup>76</sup>	<a href="https://funannotate.readthedocs.io/en/latest/">https://funannotate.readthedocs.io/en/latest/</a>
RepeatMasker	Smit et al. <sup>109</sup>	<a href="https://www.repeatmasker.org/">https://www.repeatmasker.org/</a>
AUGUSTUS v3.3.3	Stanke et al. <sup>110</sup>	<a href="https://bioinf.uni-greifswald.de/augustus/">https://bioinf.uni-greifswald.de/augustus/</a>
GeneMark-ES v. 4.33	Besemer et al. <sup>111</sup>	<a href="http://exon.gatech.edu/GeneMark/">http://exon.gatech.edu/GeneMark/</a>
Snap	Korf <sup>112</sup>	<a href="https://github.com/KorfLab/SNAP">https://github.com/KorfLab/SNAP</a>
GlimmerHMM v3.0.4	Majoros et al. <sup>113</sup>	<a href="https://ccb.jhu.edu/software/glimmerhmm/">https://ccb.jhu.edu/software/glimmerhmm/</a>
EvidenceModeler v1.1.1	Haas et al. <sup>114</sup>	<a href="https://evidencemodeler.github.io/">https://evidencemodeler.github.io/</a>
InterProScan5-48-83.0	Jones et al. <sup>115</sup>	<a href="https://interproscan-docs.readthedocs.io/en/latest/UserDocs.html">https://interproscan-docs.readthedocs.io/en/latest/UserDocs.html</a>
emapper v2.1.6-23	Huerta-Cepas et al. <sup>116</sup>	<a href="https://github.com/eggnogdb/eggno-mapper">https://github.com/eggnogdb/eggno-mapper</a>
SignalP	Almagro Armenteros et al. <sup>117</sup>	<a href="https://services.healthtech.dtu.dk/service.php?SignalP-5.0">https://services.healthtech.dtu.dk/service.php?SignalP-5.0</a>
Phobius v.1.01	Käll et al. <sup>118</sup>	<a href="https://phobius.sbc.su.se/instructions.html">https://phobius.sbc.su.se/instructions.html</a>
HMMER v3.3	Eddy et al. <sup>119</sup>	<a href="http://hmmer.org/">http://hmmer.org/</a>
dbCAN2 v9.0	Zhang et al. <sup>120</sup>	<a href="https://bcbl.unl.edu/dbCAN2/">https://bcbl.unl.edu/dbCAN2/</a>
fungiSMASH v5.2	Blin et al. <sup>121</sup>	<a href="https://fungismash.secondarymetabolites.org/#">https://fungismash.secondarymetabolites.org/#</a>
BlastKOALA	Kanehisa et al. <sup>122</sup>	<a href="https://www.kegg.jp/blastkoala/">https://www.kegg.jp/blastkoala/</a>
BUSCO	Seppely et al. <sup>123</sup>	<a href="https://busco.ezlab.org/busco_userguide.html">https://busco.ezlab.org/busco_userguide.html</a>
CATAStrophy	Livingstone et al. <sup>124</sup>	<a href="https://github.com/ccdmb/catastrophy">https://github.com/ccdmb/catastrophy</a>
BUSCO_phylogenomics pipeline	McGowan et al. <sup>125,126</sup>	<a href="https://github.com/jamiemcg/BUSCO_phylogenomics">https://github.com/jamiemcg/BUSCO_phylogenomics</a>
MUSCLE	Edgar <sup>127</sup>	<a href="https://www.drive5.com/muscle/">https://www.drive5.com/muscle/</a>
TrimAl	Capella-Gutiérrez et al. <sup>128</sup>	<a href="http://trimal.cgenomics.org/">http://trimal.cgenomics.org/</a>
IQ-TREE	Minh <sup>129</sup>	<a href="http://www.iqtree.org/">http://www.iqtree.org/</a>
iTol v6	Letunic et al. <sup>130</sup>	<a href="https://itol.embl.de/">https://itol.embl.de/</a>
R. v. 4.1.1	R Core Team <sup>131</sup>	<a href="https://www.r-project.org/">https://www.r-project.org/</a>

**RESOURCE AVAILABILITY**

**Lead contact**

Further information and requests for resources and commercial reagents should be directed to and will be fulfilled by the lead contact, Hassan Salem ([hassan.salem@tuebingen.mpg.de](mailto:hassan.salem@tuebingen.mpg.de)).

**Materials availability**

This study did not generate new unique reagents.

**Data and code availability**

- Genomic and metagenomic sequencing data generated in this study have been deposited at the National Center for Biotechnology Information (NCBI) and are publicly available as of the date of publication under BioProject PRJNA859648.
- Accession numbers are listed in the [key resources table](#).
- This paper does not report original code. Any additional information required to reanalyze the data reported in this paper is available from the [lead contact](#) upon request.

## EXPERIMENTAL MODEL AND SUBJECT DETAILS

### Insect rearing

A laboratory culture of *Chelymorpha alternans* is continuously maintained at the Max Planck Institute for Biology in Tübingen, Germany. The insects are reared in mesh containers (30 x 30 x 35 cm) along with their host plant, *Ipomoea batatas*. Experiments were conducted in climate chambers at a constant temperature of 26°C, humidity of 60%, and long light regimes (14:30h/9:30h light/dark cycles).

### Plant rearing

*Ipomoea batatas* (cv. Bauregard) plants were propagated via slip production and maintained in the greenhouse at 26°C and long light regimes (14:30h/9:30h light/dark cycles). Slips were generated by clipping terminal branches containing at least 2 well developed leaves and maintaining them in water until visible roots appeared. Slips were subsequently potted in soil.

### Microbial strain maintenance

After initial isolation, *C. alternans*-associated *F. oxysporum* is maintained on Potato Dextrose Agar at room temperature.

## METHOD DETAILS

### Scanning electron microscopy

*C. alternans* pupae and recently-eclosed adults were fixed in 2.5% (w/v) glutaraldehyde in phosphate buffered saline for 1 hour at room temperature followed by 4°C. Samples were post-fixed with 1% (w/v) osmium tetroxide for 1 hour on ice. Subsequently, samples were dehydrated in a graded ethanol series followed by critical point drying (CPD300, Leica Microsystems) with CO<sub>2</sub>. Finally, the cells were sputter-coated with a 6 nm thick layer of platinum (CCU-010, Safematic) and examined with a field emission scanning electron microscope (Regulus 8230, Hitachi High Technologies) at an accelerating voltage of 3 kV.

### Metagenome sequencing, assembly, and taxonomic assignment

Five pupae collected from five parental lineages were euthanized by freezing at –20°C for 15 minutes, then submerged in liquid nitrogen and crushed using sterile pestles. DNA was purified using the QIAGEN DNeasy Blood & Tissue Kit (Hilden, Germany) according to the manufacturer's instructions. Genomic DNA was sheared to an average size of 300 bp on a Covaris S2 Focused-Ultrasonicator. Sheared DNA was bead-cleaned up using SPRI beads (Beckman Coulter; California, USA). DNA library was constructed using the NEBNext Ultra II DNA Library Prep Kit for Illumina (Massachusetts, USA) following manufacturer's instructions. Library concentration was measured using the Qubit 1X dsDNA HS Assay Kit (Thermo Fisher PN: Q33231) on a Qubit 2.0 fluorometer and size distribution was assessed on an Agilent 2100 Bioanalyzer using the Agilent High Sensitivity DNA Kit (California, USA). Sequencing was performed inhouse on a HiSeq 3000 Sequencing System from Illumina, using the paired-end 150 bp technology and at a depth of ~100 million reads. Adaptor sequences were trimmed with Trimmomatic v0.03<sup>107</sup> using the default parameters. Reads were screened for small subunit ribosomal RNA gene (SSU rRNA) sequences and assembled using phyloFlash.<sup>46</sup> In short, reads were aligned against the filtered SSU Ref NR99 database from the SILVA release 138, with a minimum sequence identity of 70%. Taxonomical affiliation was assigned for each pair of reads by selecting the last common ancestor (LCA) of the taxonomy strings of all the database hits, as per the SILVA taxonomy. The counts of LCA consensus taxa for the library were summarized at genus level. Read assembly was performed using SPAdes under default parameters,<sup>108</sup> and subsequent contigs were screened for SSU rRNA sequences with HMM models. The final dataset is composed of SSU rRNA sequences that pass an E-value cutoff of 10<sup>-100</sup>.

### Isolation of *Chelymorpha alternans*-associated *Fusarium oxysporum*

A single strain of *F. oxysporum* was independently and consistently isolated from the surfaces of 10 *C. alternans* pupae. Sterile forceps were used to collect the white aggregations forming on the pupal surface ahead of cultivation on potato dextrose agar plates (PDA: 4 g potato starch, 20 g dextrose, 15 g agar, and distilled water up to 1 L). The only microbe consistently propagating on plate was *F. oxysporum*, as corroborated by sequencing the microbe's internal transcribed spacer (ITS) rDNA and the translation elongation factor 1- $\alpha$  (Tef-1 $\alpha$ ) genes. The ITS sequence perfectly aligned to the ribosomal sequences retrieved from the metagenomic assembly outlined above.

### Diagnostic PCR screening

The presence of *F. oxysporum* throughout host development (eggs, larvae, pupae and adults) was assessed using diagnostic PCR from four *C. alternans* parental lineages. DNA was purified from the outer surfaces of all developmental stages using the QIAGEN DNeasy Blood & Tissue Kit (Hilden, Germany). Diagnostic PCR was performed using *F. oxysporum*-specific primers (Fwd: 3'-GGTATCGACAAGCGAACCAT-5', Rev: 3'-TAGTAGCGAGGAGTCTCGAA-5') targeting the symbiont's Tef-1 $\alpha$  gene. PCR amplifications were conducted on an Analytik Jena Biometra TAdvanced Thermal Cycler using a final volume of 20  $\mu$ l containing 1  $\mu$ l of DNA template, 0.5  $\mu$ M of each primer, and 2X DreamTaq Green PCR Master Mix. The following cycle parameters were used: 5 min at 95°C, followed by 34 cycles of 95°C for 30s, 58°C for 30s, 72°C for 1 min, and a final extension time of 2 min at 72°C.

### Quantitative PCR

The relative abundance of *F. oxysporum* (live and recently dead cells) was estimated across pupal development by quantifying Tef-1 $\alpha$  gene copy numbers using an Analytik Jena qTOWER<sup>3</sup> cyclor. Tef-1 $\alpha$  was chosen given its single copy within the genome of *F. oxysporum*, and its stable expression dynamics.<sup>132</sup> DNA was purified as described above from 18 pupae collected from three different *C. alternans* parental lineages and spanning each of the six days required for the insect to undergo metamorphosis. The final reaction volume of 25  $\mu$ l included the following components: 1  $\mu$ l of DNA template, 2.5  $\mu$ l of each primer (10  $\mu$ M) (Fwd: 3'-GGTATC GACAAGCGAACCAT-5', Rev: 3'-TAGTAGCGAGGAGTCTCGAA-5'), 6.5  $\mu$ l of autoclaved distilled H<sub>2</sub>O and 12.5  $\mu$ l of ThermoFischer SYBR Green Mix. Primer specificity was verified *in silico* by comparison with reference fungal sequences in NCBI. Additionally, PCR products were sequenced to confirm primer specificity *in vitro*. Standard curves (10-fold dilution series from 10<sup>-1</sup> to 10<sup>-8</sup> ng/ $\mu$ l) were generated using purified PCR products and measuring their DNA concentration using a NanoDropTM1000 spectrophotometer. The following cycle parameters were used: 95°C for 10 min, followed by 45 cycles of 95°C for 15s, 58°C for 45s, and a melting curve analysis was conducted by increasing temperature from 60°C to 95°C within 30s. Based on the standard curve, absolute copy numbers were calculated, which were then used to extrapolate symbiont relative abundance by accounting for the single copy of the Tef-1 $\alpha$  gene in *F. oxysporum*'s genome.

Six newly-eclosed adults were collected from three different *C. alternans* parental lineages to determine the abundance of *F. oxysporum* in adult beetles relative to their legs. DNA was purified from three whole insects, as well as legs that were dissected from the remaining three samples. Symbiont abundance was estimated by quantifying Tef-1 $\alpha$  gene copy numbers as described above.

### Symbiont genome sequencing, assembly, and annotation

High molecular weight genomic DNA was extracted as described by Penouilh-Suzette et al.<sup>133</sup> Fungal suspensions were obtained by adding PBS to fungal plates and gently scraping off the surface with a spreading handle. Following centrifugation for 3 minutes at full speed and removal of the supernatant, fungal material was grounded in liquid nitrogen with a pestle, resuspended in lysis buffer, and vortexed at full speed for 30 seconds. At this point, Proteinase K was incorporated, and the DNA extraction was further carried out as per the original protocol. The extracted DNA was sheared to between 15 kb and 20 kb using the Megaruptor 2 (Diagenode). A HiFi sequencing library was prepared using SMRTbell Express Template Prep Kit 2.0 (PN 101-853-100). The library was further size selected electrophoretically using the BluePippin Systems from SAGE Science. The appropriate fractions for sequencing runs were identified on the Femto Pulse System (Agilent). After pooling the desired size fractions, the final library was purified further and concentrated using AMPure PB beads (Pacific Biosciences PN:100-265-900). Finally, the library was checked for concentration using Qubit 1X dsDNA HS Assay Kit (Thermo Fisher PN: Q33231) and final size distribution was confirmed on the Femto Pulse. Sequencing was performed using one 8M SMRT cell on the PacBio Sequel II System at the Max Planck for Biology.

High Fidelity (HiFi) reads (>Q20) were generated using the circular consensus sequencing analysis method by the pbbccs tool from the pbbioconda package (-min-passes 3 -min-rq 0.99 -min-length 10 -max-length 50000). Gene prediction and annotation was performed using the Funannotate v.1.8.3 pipeline.<sup>134</sup> Repeats were identified with and soft masked using RepeatMasker.<sup>109</sup> Protein evidence from a UniprotKB/Swiss-Prot-curated database was aligned to the genome using TBlastN and Exonerate. Four gene prediction tools were used: AUGUSTUS v3.3.3,<sup>110</sup> GeneMark-ES v. 4.33,<sup>111</sup> Snap,<sup>112</sup> and GlimmerHMM v3.0.4.<sup>113</sup> tRNAs were predicted with tRNAscan-SE (48-83.0). To calculate the set of consensus gene models for the genome, the generated gene prediction models were passed to EvidenceModeler v1.1.1.<sup>114</sup> Functional annotation was obtained using BlastP to search the Uniprot/SwissProt protein database (v2021\_01).<sup>135</sup> Protein families (Pfam) and Gene Ontology (GO) terms were assigned with InterProScan5-48-83.0.<sup>115</sup> Additional predictions were inferred by alignments to the eggNOG 5 orthology database,<sup>136</sup> using emapper v2.1.6-23.<sup>116</sup> The secretome was predicted using SignalP,<sup>117</sup> and Phobius v.1.01,<sup>118</sup> which identifies proteins carrying a signal peptide. Carbohydrate-active enzymes were identified using HMMER v3.3<sup>119</sup> and family specific HMM profiles from dbCAN2 v9.0.<sup>120</sup> Proteases and protease inhibitors were predicted using the MEROPS database v12.0,<sup>137</sup> and biosynthetic gene clusters were annotated using fungiSMASH v5.2<sup>121</sup> with relaxed parameters. Protein-coding genes were further annotated by mapping them against the KEGG pathway database using BlastKOALA.<sup>122</sup> Benchmarking Universal Single-Copy Orthologs were identified with BUSCO2.<sup>123</sup> Fungal virulence factors were identified by blasting the final proteome against the Pathogen-Host Interactions database.<sup>138</sup>

To infer the trophic position of the fungal symbiont relative to its arsenal of encoded hydrolases, a CATASrophy analysis<sup>124</sup> was performed on the HMM profiles of annotated carbohydrate-active enzymes (CAZymes) and against the dbCAN v10 database.<sup>79</sup> CAZyme HMM profiles from the fungal symbiont were compared to those of 133 fungal species and 15 oomycetes that had a trophic classification assigned to them, employing a multivariate analysis. Centroids were calculated for each trophic class and relative centroid distances (RCD) were estimated for each species. The closest centroid was assigned an RCD score of 1, and the furthest a score of 0. Every other centroid distance was expressed as a relative proportion.

### Phylogenetic reconstruction

Genomes from representative ascomycete lineages were used to reconstruct the phylogenetic relationship between the symbiont of *C. alternans* and its fungal relatives using the BUSCO\_phylogenomics pipeline.<sup>125,126</sup> Single copy orthologues spanning 80 genomes were identified by running BUSCO v5<sup>123</sup> with the Ascomycota\_odb10 lineage database. The analysis identified 180 single-copy orthologs shared by all ascomycete lineages in the dataset, including members of the *F. oxysporum* species complex. Gene sequences

were aligned with MUSCLE<sup>127</sup> and the alignment was trimmed with TrimAl.<sup>128</sup> Output alignments were concatenated into a supermatrix. A Maximum Likelihood tree was built with IQ-TREE<sup>129</sup> allowing ModelFinder<sup>139</sup> to predict the best evolutionary model for the partitioned alignment. The resulting tree was rooted at midpoint and visualized with iTol v6.<sup>130</sup>

### Symbiont manipulation and survival assays

To assess the efficacy of the symbiont manipulation procedure, sixteen pupae were collected from eight different *C. alternans* parental lineages, representing eight replicates, and separated into two experimental treatments: (i) untreated control, and (ii) individuals treated with benzimidazole, a fungicide. The latter group was generated by twice applying 100  $\mu$ l 0.5% (w/v) benzimidazole solution (5 g/100 ml dH<sub>2</sub>O) over 1- and 2-day-old pupae. Following four-day incubations at room temperature, DNA was purified from both treatments using the QIAGEN DNeasy Blood & Tissue Kit (Hilden, Germany) according to the manufacturer's instructions. The relative abundance of *F. oxysporum* was estimated by quantifying Tef-1 $\alpha$  gene copy numbers using an Analytik Jena qTOWER<sup>3</sup> cyclor as described above (diagnostic PCR screening section).

To assess the impact of the symbiont-clearing procedure on pupal development, 46 pupae were collected from six *C. alternans* parental lineages, representing six replicates. Individuals were then separated into two experimental treatments, as described above: untreated control, and individuals treated with benzimidazole. Pupae were observed daily and adult eclosion rates were recorded.

Field experiments were conducted in Gamboa, Republic of Panamá (N: 9°07'12.5; W: 79°41'46.0), to assess the protective properties of *F. oxysporum* for its beetle host in its natural environment. Pupae collected from five *C. alternans* parental lineages (98 in total), representing five replicates, were separated into the following experimental treatments: untreated pupae, and individuals treated with benzimidazole, as described above. Both groups were then divided into experimental cages that were either exposed or sealed to prevent entry by ants, predatory bugs, and other arthropods. Pupae were monitored daily, and survivorship rates were recorded for four days.

### Beetle propagation of *F. oxysporum* to the sweet potato plant

To test whether *C. alternans* can vector *F. oxysporum* to its host plant, we confined 2 newly-eclosed adult beetles together with 10 *F. oxysporum*-free sweet potato plants (*I. batatas*). Infection frequencies were compared to 10 *I. batatas* grown in the absence of *C. alternans*. All groups were maintained in climate chambers at a constant temperature of 26°C, humidity of 60%, and long light regimes (14:30h/9:30h light/dark cycles). Following a four-week incubation period, we applied diagnostic PCR to assess the presence of *C. alternans*-associated *F. oxysporum* in leaf tissue. Leaves were collected, ground in liquid nitrogen, and homogenized. DNA was purified using the DNeasy Plant Mini Kit (Hilden, Germany) according to the manufacturer's instructions. Diagnostic PCR was performed using *F. oxysporum*-specific primers (Fwd: 3'-GGTATCGACAAGCGAACCAT-5', Rev: 3'-TAGTAGCGAG GAGTCTCGAA-5') targeting the symbiont's Tef-1 $\alpha$  gene and as described above (diagnostic PCR screening section).

### Phytopathogenicity of *F. oxysporum*

A total of 27 *I. batatas* plants were grown for three weeks prior to treatment. Symbiotic *F. oxysporum* was cultured overnight in potato dextrose broth at 26°C and resuspended in PBS at a concentration of 10<sup>9</sup> spores/ml. 15 plants were inoculated with a 100  $\mu$ l droplet of the fungal suspension (i.e., 5 $\times$ 10<sup>4</sup> spores in total), and 12 were treated with the same volume of PBS as a control.<sup>140</sup> All groups were maintained in the greenhouse for 21 days at a constant temperature of 20°C and long light regimes (14:30h/9:30h light/dark cycles). Disease progression was monitored daily, and symptoms were scored according to the Yellow Wilt Disease Test. To determine the extent of pathogen colonization, a trypan blue exclusion test was performed using leaves from both treatments. Briefly, leaves were boiled in a lactophenol-trypan blue solution (10 mL lactic acid, 10 mL glycerol, 10 mg phenol, and 10 mg trypan blue dissolved in 10 mL distilled water) for 1 min and then cleared with chloral hydrate (2.5 g mL<sup>-1</sup>) overnight. Leaves were then examined under a dissection scope to determine the extent of viable (clear) versus nonviable (blue) cells.<sup>71</sup>

### QUANTIFICATION AND STATISTICAL ANALYSIS

All statistical analyses were carried out in R. v. 4.1.1.<sup>131</sup> Fungal symbiont population dynamics during pupal development were analyzed using a general linear model, after reverse transformation and validation of a normal distribution, and using time as a fixed factor. Differences in fungal abundance between different time points were analyzed with a Tukey HSD post-hoc test and Bonferroni correction for multiple comparisons. A non-parametric Wilcoxon rank sum test was employed to assess the effect of benzimidazole application on the abundance of *F. oxysporum* growing on pupae. A generalized linear model with a binomial error structure and a logit-link function was employed to investigate differences in adult eclosion rate following benzimidazole treatment, and the prop.test() function was used to obtain the 95% binomial confidence intervals. Survival rates were analyzed across the different treatments with a log-rank test and a proportional hazards regression (package *survival* with functions survdiff() and coxph(), respectively),<sup>141</sup> and visualized by computing a Kaplan-Meier curve, with the function survfit(). Differences in survivorship between groups were calculated with a post-hoc analysis using the function pairwise\_survdiff(), and Bonferroni correction for multiple comparisons. Pearson's  $\chi^2$  tests were performed to assess differences in (i) *F. oxysporum* infection frequencies in sweet potato plants (*Ipomoea batatas*) grown in the presence and absence of *Chelymorpha alternans*, and (ii) the proportion of *I. batatas* plants exhibiting disease symptoms after inoculation with *F. oxysporum* compared to non-inoculated plants. The prop.test() function was also used to obtain

the 95% binomial confidence intervals for these binomial distributions. After testing for data normality, a general linear model was used to assess differences in the abundance of *F. oxysporum* in adult beetles relative to their legs, using body part as a fixed factor. Plots were generated with the package `ggplot2`.<sup>142</sup>

Further statistical details for each test (e.g. exact value of *n*, meaning of *n*, precision measures, etc.) can be found in the main text and figure legends. For every statistical analysis significance was defined as a  $p \leq 0.05$ .